ROBUST COPPER BRAZE FOR HERMETIC SEALING OF SOLID OXIDE FUEL CELLS

by

Danielle Elizabeth Ator

A thesis submitted in partial fulfillment
of the requirements for the degree

of

Master of Science

in

Mechanical Engineering

MONTANA STATE UNIVERSITY
Bozeman, Montana

July 2008

APPROVAL

of a thesis submitted by

Danielle Elizabeth Ator

This thesis has been read by each member of the thesis committee and has been found to be satisfactory regarding content, English usage, format, citation, bibliographic style, and consistency, and is ready for submission to the Division of Graduate Education.

Stephen W. Sofie, Ph.D.

Approved for the Department of Mechanical Engineering

Christopher H. M. Jenkins, Ph.D.

Approved for the Division of Graduate Education

Dr. Carl A. Fox

STATEMENT OF PERMISSION TO USE

In presenting this thesis in partial fulfillment of the requirements for a master's degree at Montana State University, I agree that the Library shall make it available to borrowers under rules of the Library.

If I have indicated my intention to copyright this thesis by including a copyright notice page, copying is allowable only for scholarly purposes, consistent with "fair use" as prescribed in the U.S. Copyright Law. Requests for permission for extended quotation from or reproduction of this thesis in whole or in parts may be granted only by the copyright holder.

Danielle Elizabeth Ator

July 2008

ACKNOWLEDGEMENTS

I would like to begin by expressing my deepest thank you to Dr. Stephen Sofie for being my mentor throughout the course of this research. It was Dr. Sofie's knowledge and spirit that kept me motivated and determined throughout my course of study. I am greatly honored to be able to say that I was able to learn from a professor who expresses such love and devotion for the field of materials engineering.

I would like to acknowledge Johannes Brusher, whose initial work in brazing served as an excellent reference and starting point for my research and Ammon Palmer who helped set up test equipment and trouble shot electrical problems throughout the brazing study. Deep gratitude goes to Dr. Sarah Codd and Dr. David Miller for their excellent support as committee members. I thank you both for your time and input. Finally, I would like to thank my friends and family, I would not be where I am today if it were not for their love and support. This work was supported by the MSU-HiTEC program. MSU-HiTEC is funded by the United States Department of Energy under Award No. DE-AC06-76RL01830. However, any opinions, findings, conclusions or recommendations expressed herein are those of the author(s) and do not necessarily reflect the views of the DOE.

TABLE OF CONTENTS

TABLE OF CONTENTS -- CONTINUED

TABLE OF CONTENTS -- CONTINUED

LIST OF TABLES

Table Page

LIST OF FIGURES

Figure Page

LIST OF FIGURES -- CONTINUED

Figure Page

LIST OF FIGURES -- CONTINUED

Figure Page

LIST OF EQUATIONS

Equation Page

Nomenclature

Ag……...Silver

Al……Aluminum

ALT…….....Aluminum Titanium Oxide, Aluminum Titanate

ASC.....Anode Supported Cell

Au……...Gold

Cr……Chromium

CTE……Coefficient of Thermal Expansion

Cu……...Copper

DTA……Differential Thermal Analysis

EDS……Energy Dispersive x-ray Analysis

ESC……Electrolyte Supported Cell

FEM……Field Emission scanning electron Microscopy

k_l .....Rate of linear oxidation

k_p .....Rate of parabolic oxidation

L_o .....Initial sample length

MEK……...Methyl Ethyl Ketone

Mo……...Molybdenum

MSU……...Montana State University

Nb……...Niobium

Ni……Nickel

NPT……National Pipe Thread

Pd……...Palladium

Pt……Platinum

psi……...Pounds per square inch

RAB……...Reactive Air Brazing

Si……Silicon

SOFC……..Solid Oxide Fuel Cell

SS……....Stainless Steel

TGA……....Thermal Gravimetric Analysis

Ti…….....Titanium

TiSi……..Titanium Silicide

V.....Vanadium

V_r …….....Volume of reinforcement

V_m …….....Volume of matrix

YSZ……..Yttria Stabilized Zirconia

Zr……...Zirconia

α_c …….CTE of composite

α_l .....Linear Coefficient of Thermal Expansion

α_r …….....CTE of reinforcement

α_m ……CTE of matrix

ΔL .....Change in length

Δ_m .....Change in mass

ΔT .....Change in temperature

γ_{LG} .....Force between liquid and gas phase

γ_{SG} .....Force between solid and gas phase

γ_{SL} .....Force between solid and liquid phase

θ_c .....Wetting contact angle

ABSTRACT

Solid oxide fuel cells (SOFCs) are becoming of increasing interest as a primary power source in today's industrial market. The voltage of a single cell under load is approximately 0.7 volts necessitating the use of many cells in series to generate useful electrical potentials, which gives rise to the SOFC stack. One of the key technical challenges in improving the long term performance and reliability of stacks is in the effective sealing of stack interfaces, particularly in planar stacks for which a hot seal (700-900ºC) is required. SOFC stack seals must be: resistant to oxidation/volatilization in oxidizing and reducing atmospheres, must wet and bond to the joining members (both ceramic and metal), form a hermetic seal to prevent hydrogen leakage, and have a coefficient of thermal expansion (CTE) close to that of the adjoining components to limit thermally induced stresses.

Active metal copper-based brazes present a novel approach to sealing SOFCs by means of robust mechanical/thermal properties providing strong, hermetic braze-interconnect and braze-YSZ interfaces. A commercially available active braze alloy utilizing no precious metal additives was tested and compared to custom synthesized braze compositions fabricated and tested at MSU. Two testing configurations were evaluated for this sealing study, utilizing dense YSZ substrates joined to 25.24mm, 430SS coupons as well as 25mm 440SS pressure test fixtures. Active braze alloys require a protective atmosphere to facilitate chemical bonding with YSZ and results show excellent performance in moderate vacuum (10^{-4} to 10^{-5} mbar) and argon atmosphere. Sample characterization was performed by electron microscopy, energy dispersive x-ray spectroscopy, pressurized rupture and leak tests, differential thermal analysis, thermal gravimetric analysis and thermodynamic evaluation.

Robust copper-based brazes show potential for the use of sealing in SOFC applications. The brazes display desirable characteristics for sealing applications including the formation of chemically bonded braze joints, formation of a protective oxide barrier and high strength properties. Evidence of silicon diffusion into the YSZ may be problematic for long-term SOFC operation, however, development of a silicon-free braze has yielded excellent performance near that of the commercially available brazing powder.

INTRODUCTION

Copper Based Braze Research Motivation

Solid oxide fuel cells (SOFCs) are becoming of increasing interest as a primary power source in today's industrial market due to a number of advantages including: high efficiency, low emissions and potential use in a wide range of applications. A single SOFC does not provide enough power for most applications; as a result, individual cells are connected in series to increase the power output, forming a SOFC stack. [1,2]

One of the key technical challenges in improving the long term performance and reliability of solid oxide fuel cell stacks is in the effective sealing of stack interfaces. While tubular designs of SOFCs are able to utilize a cold seal, planar SOFC designs must employ a hot seal for effective sealing, which is the focus of this research. Active metal copper based brazes present a novel approach to sealing planar SOFC stacks by means of robust mechanical/thermal properties providing strong, hermetic braze-interconnect and braze-YSZ interfaces.

Brazing for SOFC applications must fulfill many requirements. The primary requirement for a planar braze seal is to maintain corrosion resistance at SOFC operating temperature (700-900 ºC) in both an oxidized and reduced environment. The metallic braze must also have a coefficient of thermal expansion (CTE) close to that of the adjoining components to avoid residual stresses induced during thermal cycling. These residual stresses can pre-damage the SOFC components, shortening the life of the cell. Finally, braze seals must wet and bond to the joining members, providing a crack free,

hermetic joint which remains durable at elevated temperatures and mechanically stable during operation. [1,3]

BACKGROUND

Solid Oxide Fuel Cell Stacks

The typical power output for a single SOFC is approximately 0.7 volts, which is minimal in comparison to power consumption for most consumer products. To obtain power output sufficient for commercial applications, individual cells must be combined in electrical series forming an SOFC stack.

Stack Geometries

There are two primary SOFC stack designs that have become common place in SOFC technology, a tubular design and a planar design. Each of the SOFC stack geometries yields certain strengths and weaknesses, for which the advantages and disadvantages to each are discussed in the sections below.

Tubular SOFC Designs: The design of a tubular SOFC consists of many small tubes connected in series. While different tubular designs are utilized, one commonly implemented tubular design consists of an anode at the center of the tube, a cathode around the outer portion of the tube and an electrolyte located in between. The tubular design is desirable over the planar stack design because the geometry of this design does not require the use of high temperature, gas tight seals to contain the reactive gases of the cell. Hermetic seals are desired, however, cold seals can be used. Unfortunately, high production costs and most notably the limitations for which long tubes can be effectively packed yield lower power density, making the tubular design less desirable. [4]

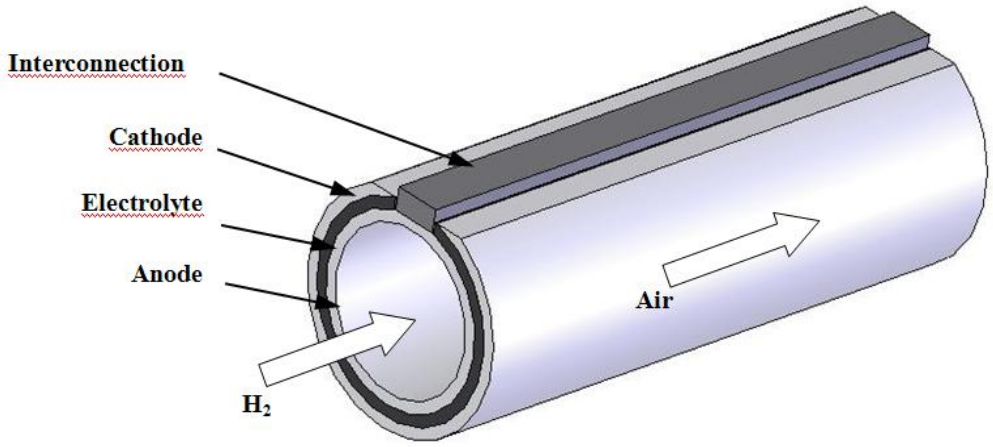

Figure 1 Design of a Tubular Solid Oxide Fuel Cell [3]

Planar SOFC Designs: The planar SOFC design allows for simple manufacturing and more effective volumetric stacking of cells which allows for increased power density (greater than 400 $^{mW}/_{cm^2}$) and specific power density (greater than 0.2 $^{kW}/_{kg}$). The planar SOFC design requires a robust hermetic seal to contain the reactive gases of the SOFC. The braze seal must bond to both metal and ceramic SOFC components and operate successfully at elevated temperatures. Funding for this project was provided through the MSU-HiTEC program (High Temperature Electrochemistry Center). The focus of this program is the development of planar SOFC stack technology which has a 40,000 hour life span with no more than 1% degradation per 1000 hours at a cost of $400 per kW. The complex nature of the development of a successful planar SOFC seal is the leading drawback of the planar SOFC stack design. [4]

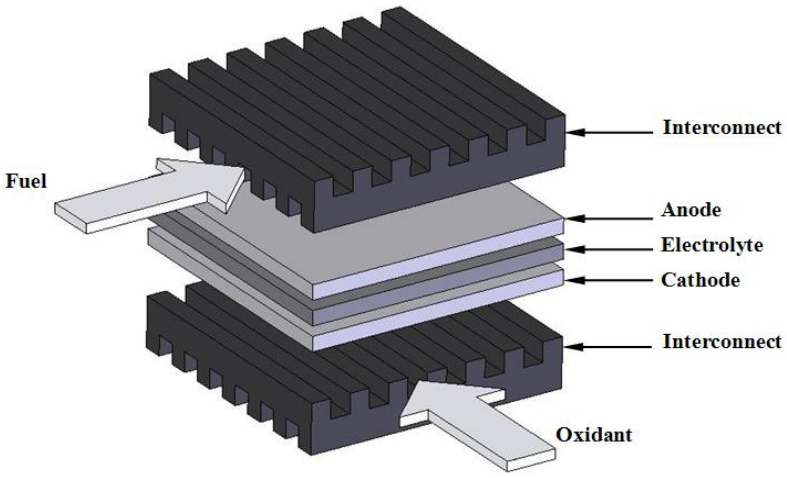

Figure 2 Design of a Planar Solid Oxide Fuel Cell [3]

Sealing Of Solid Oxide Fuel Cells

As previously mentioned, one of the key technical challenges in the development of a successful planar SOFC stack is the development of an effective seal at the SOFC stack interfaces. The primary purpose of the SOFC seal is to prevent the mixing of the fuel and air outside of the reactive zone of the SOFC while also preventing the leaking of the gases from the SOFC stack. Due to the fact that SOFCs operate in a temperature range between 600 ºC and 900 ºC it is important to note that the auto-ignition temperature of hydrogen (one of the primary gases used in the fuel cell) and air is approximately 350 ºC, thus yielding instantaneous ignition of fuel.

The seal for an SOFC stack must fulfill the following requirements: maintain corrosion resistance at working temperature in both an oxidized and reduced environment, have no electrical conductivity, wet and bond to the joining members, provide a crack free joint, form a hermetic seal, have a CTE close to that of the adjoining members in order to avoid residual stresses, have high adhesion strength, maintain

durability at elevated temperatures and during thermal cycling and maintain mechanical stability during operation.

State-of-the-art SOFC technology currently utilizes vitreous (amorphous and hence viscous) glass seals, however, much research is being conducted in the use of metals for SOFC braze seal applications.

Glass Seals

There are two primary types of glass seals currently being evaluated in SOFC development: self-healing compliant glasses and glass ceramics. Glass was initially selected as the sealing material for SOFCs as it is easy to make and apply. Glasses are ideal at increased temperature, as they become viscous and easy to work with and manipulate. However, glass seals devitrify (crystallize) over time, thus becoming rigid under high temperature thermal cycling making the glass seals brittle and vulnerable to stress induced cracking [5]. The glasses also leach iron and chromium from the stainless steel, further increasing the rate of devitrification and hence compromising the chemical stability of the seal.

Self-Healing Compliant Glasses: A self-healing compliant glass is an amorphous, viscous glass that is able to withstand small stresses and cracks. Further, under proper operation defects from thermal cycling are essentially repaired in-situ, thus sealing leaks that would otherwise destroy an entire stack. This type of glass does not fully crystallize, and is required to remain amorphous for the entire operation life of the seal. The glass is heated to a temperature close to that of the melting temperature (which may also coincide with SOFC operation temperature) and small cracks introduced during thermal cycling

are removed through the amorphous nature of the glass. This sealing medium works well for short term applications, however, over time a self-healing glass has a tendency to crystallize. The CTE of the glass seal is also dictated by the extent of crystallization, therefore the thermal stress of an amorphous glass going through a crystallization process is in constant flux; a characteristic not desirable in SOFCs. Ultimately, this crystallization leads to the loss of the self-healing feature and makes the glass seal vulnerable to stress related cracking, inducing leaks into the once hermetic seal. [5,6]

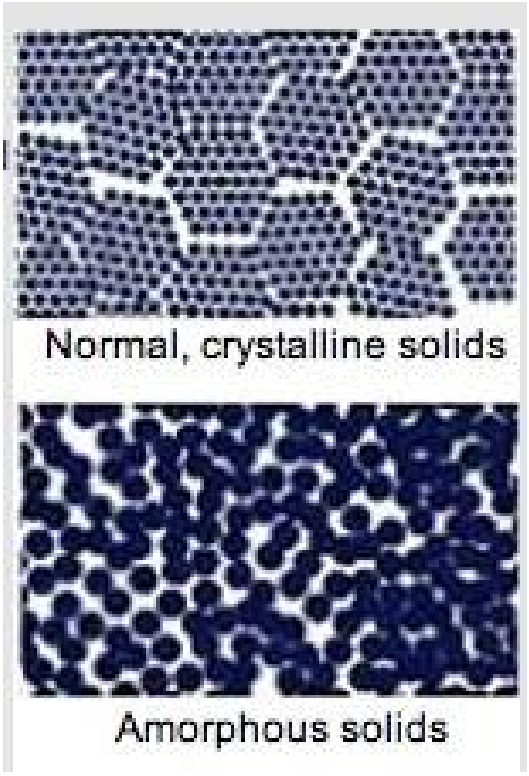

Figure 3 Microstructure of Crystalline Solid and an Amorphous Solid [7]

Glass Ceramics: A glass ceramic is a purposely crystallized glass, very rigid in nature. This type of glass is desirable as it is much stronger than most other types of glass and is unchanging over time yielding a constant CTE. However, this type of seal

offers no stress relief making it brittle and without self healing behavior, making the seal susceptible to cascading stress-related leaks. [5,6,8]

Compressive Mica: A compressive seal utilizes compressive external forces to seal together two adjoining components with a high-temperature, compliant material. Mica and mica-metal hybrid seals have shown some success in the sealing of SOFCs. Mica is more oxidation resistant than most metal powders; however, the low CTE of Mica (6.9×10^{-6}/°C), seal leakage and crystallization have proved to be problematic. Mica-metal hybrid compressive seals have been developed to improve the performance of the mica compressive seals. [5]

Metallic Braze Seals

An alternate approach for the sealing of SOFC stacks incorporates the use of metallic brazes. Metallic air brazes yield physical bonds like those of glass seals, however, active metallic brazes can yield a strong chemical bond between the braze components, providing compliant behavior for stress relief, excellent oxidation resistance and an electrical conductivity which can be modified by thermal treatment such as in active metal brazing.

Reactive Air Brazing: Reactive air brazing (RAB) is a joining technique which utilizes a reactive metal yielding a molten oxide to form a metallic joint. The strength of the metallic joint formed during RAB is dependent of the oxide scale that forms on the metal during the heating process. RAB does not require the use of a vacuum or cover-gas environment for the brazing process; however, all reactive air brazes contain precious

metal as the metal oxide needed to form the robust braze joint. Precious metals used in air brazes often include silver, gold or platinum in the form of an oxide. [9,10]

Silver-based brazes give way to oxygen and hydrogen transport due to the fact that silver conducts both oxygen and hydrogen. This process can lead to cell degradation by means of chemical reduction/oxidation of both braze additives as well as SOFC electrodes. Silver-based brazes also have high volatilization rates which can lead to thermal etching, substantial chemical interaction with chromium containing stainless steels, poor wetting with the ceramics, and no chemical bonding with the joint interfaces, giving purely a physical bond between the braze and the adjoining materials. The often expensive, precious metal additives make many air brazes undesirable for SOFC applications. [11,13]

Active Metal Brazing: Active metal brazing is the most common method used for the joining of ceramics to ceramics and ceramics to metals as it is simple, yet cost effective. [11,12] Active metal brazing is a metallurgical bonding process, which upon heating, causes an active element to react with the surfaces of the materials to be joined creating a bond during the cooling and solidification of the braze alloy. The metallic brazes usually consists of an active element such as: titanium, zirconium, vanadium, niobium or molybdenum and a filler metal or alloy to aid in the reduction of oxidation and residual stresses, such as: silver, gold, copper, nickel, palladium, platinum, or chromium. [1,13]

Although active metal brazing must take place in a vacuum or cover gas environment to prevent oxidation of the active metals, there are many other advantages to

the active metal brazing process. Active metal brazing creates a strong chemical bond to the adjoining metal and YSZ components, a characteristic unique to this method. Additionally, active metal brazing does not require the use of noble metals, which helps the good of achieving low SOFC costs, provides excellent oxidation resistance and allows for electronic conductivity to be modified by thermal treatment.

Due to its good fluidity in the molten state, excellent ductility and chemical inertness, copper is often used as a filler metal for the active metal brazing process. Copper has a high thermal conductivity (398 $^{W}/_{m}K$) and high electrical conductivity ($6.0\times10^{-7}\,\Omega^{-1}m^{-1}$) which allow for quick heat dissipation at the SOFC joint while meeting the basic electrical conductivity requirements. The large ductility found in copper can help accommodate the buildup of thermal stresses, which may develop due to the CTE mismatch of the braze material and the outlying SOFC components. The chemical inertness of copper allows for copper to be utilized at high operating temperature while exhibiting good oxidation resistance through the addition of parabolic oxide forming additives, an important property for SOFC applications. [11]

Coefficient of Thermal Expansion

The coefficient of thermal expansion is a measure of the contraction or expansion that a material undergoes as the result of thermal variation. Generally, in the case of most solids, as temperature is increased, the solid component will expand. The linear thermal expansion coefficient is a one dimensional length change as a function of temperature and is defined by the following equation:

$$\frac{\Delta L}{L_o} = \alpha_l \times \Delta T$$

Equation 1 Linear Coefficient of Expansion [14]

where ΔL is the change in length of the component, L_o is the original length of the component, α_l is the linear expansion coefficient and ΔT is the temperature change. [14]

One primary problem in the joining of oxide ceramics and metals is the mismatch of thermal expansion characteristics. Metals traditionally have thermal expansion characteristics far greater than oxide ceramics. When two adjoining materials have largely different CTEs, the two materials will expand and contract differently, introducing thermal stresses into the adjoining materials. Given the brittle nature of the core SOFC ceramic components, these thermal stresses can lead to small cracks and fractures, decreasing the performance and potentially decreasing the lifetime of the component (see Figure 4).

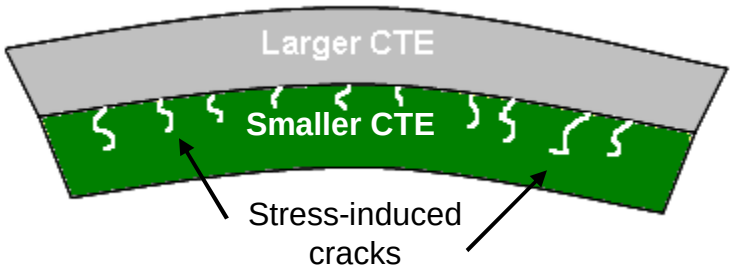

Figure 4 Schematic Showing Cracks Introduced due to CTE Mismatch

The coefficients of thermal expansion for the Copper ABA braze alloy, the MSU braze powders and the adjoining SOFC materials are shown in Table 1. Lower CTE mismatch between components means smaller stresses introduced during thermal treatment. The large CTE mismatch between the Copper ABA braze alloy and the YSZ

and stainless steel components could have substantial effects on the reliability of the SOFC stack, possibly fracturing the electrolyte of the cell or introducing leaks into the braze seal.

Table 1 Coefficient of Thermal Expansion for SOFC Materials

Material	CTE (/°C)
YSZ	9.5×10^{-6}
430SS	12.7×10^{-6}
Copper ABA	19.5×10^{-6}
Cu	16.5×10^{-6}
Si	2.6×10^{-6}
Ti	8.6×10^{-6}
Al	23.1×10^{-6}
Ag	18.9×10^{-6}

The CTE mismatch between the SOFC components and the metallic braze can be addressed in two ways, the metallic braze selected for the braze seal would need to be ductile in nature, in order to accommodate the CTE mismatch and reduce thermal stresses at the joint, or the CTE of the braze metal would need to be lowered through the addition of CTE lowering additives as alloying agents (metals) or precipitates (ceramics).

Electrical Conductivity

Electrical conductivity is an important factor in the sealing of SOFCs because an electrically conductive seal can short circuit the cell. As a result, it is imperative that the braze seal is either insulated, or not in contact with the electrodes of the SOFC. Electrical conductivity of the metallic braze seal can be shut off locally in regions where the braze metal has been bonded to an ion conductor. YSZ is engineered with oxygen vacancies to allow oxygen ions to diffuse. The oxygen ions will reach the internal braze/YSZ interface and form an aluminum oxide scale. This aluminum oxide scale will act as a

barrier shutting off the electrical conductivity in that particular region. The application of the metallic braze for SOFC's is especially designed for use in electrolyte supported cells (ESC), where brazing would be done to YSZ electrolyte lips where electrical conduction is not a problem. However, for the application of anode supported cells (ASC) in which the braze is in direct contact with the anode and cathode, the ability to shut of electrical conductivity locally is essential. Figure 5 illustrates how a braze seal is implemented for both an ESC and an ASC.

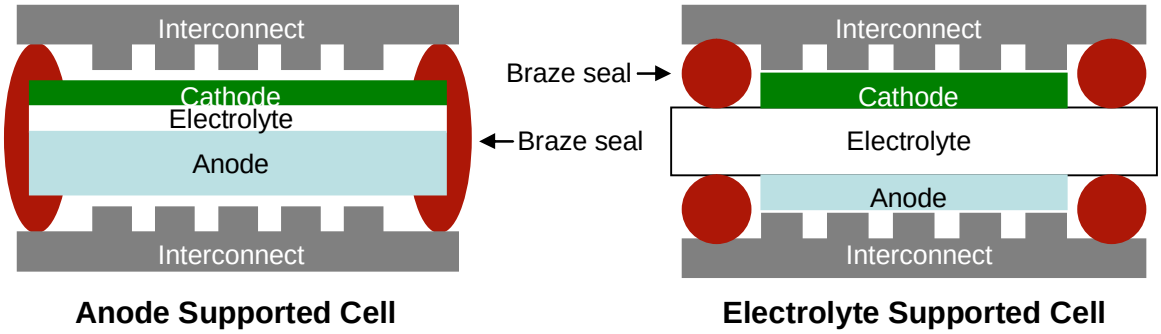

Figure 5 Braze Seal Location for ASC and ESC

Wetting Behavior

Wetting is important in the bonding of two materials. Wetting behavior is described by the contact between a liquid and a solid. The amount of wetting is dependent on the surface tensions of the interfaces involved such that the total energy is minimized or the system is in a state of equilibrium. The contact angle of the liquid is related to the net force between the various phases present. Figure 6 shows the relationship between the forces of the phases and the contact angle.

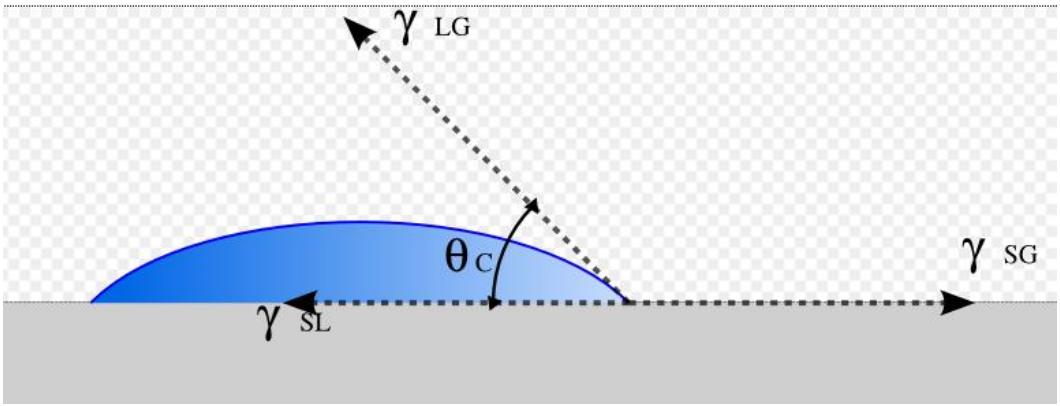

Figure 6 Wetting Relationship between Forces and Contact Angle [15]

γ_{LG} represents the force between the liquid and gas phase, γ_{SG} between the solid and gas phase and γ_{SL} between the solid and liquid phase. The contact angle can be calculated from a force balance applied at the contact point:

$$\gamma_{SG} = \gamma_{SL} + \gamma_{LG} \times \cos(\theta_c)$$

Equation 2 Wetting Contact Angle [15]

A smaller contact angle of a droplet indicates better wetting of the surface. A contact angle greater than 90° is usually considered non-wettable while a contact angle of less than 90° is considered wettable. Figure 7 displays various wetting behavior contact angles for a fluid.

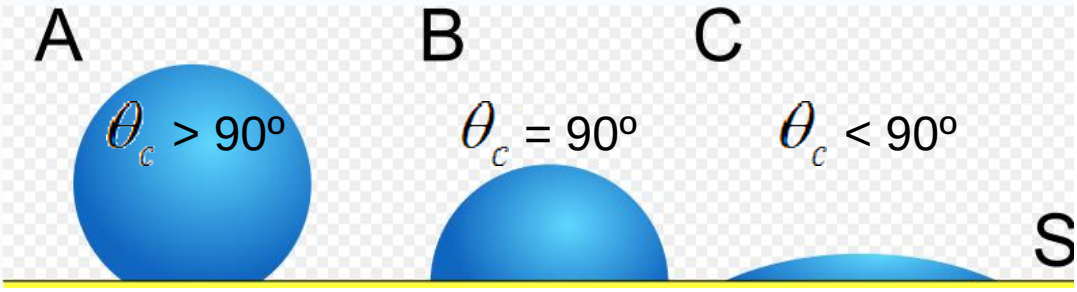

Figure 7 Wetting Behavior of Liquids on Solids [15]

Droplet A shows a liquid droplet displaying poor wetting, droplet B displays mediocre wetting and droplet C displays good wetting behavior. [15,16]

Titanium as the Active Element

Metals do not generally bond to ceramics so an active element is used to aid in the bonding process in order to obtain a metal-ceramic bond. Active elements react with oxides, carbide and/or nitrides to form wettable layers. Titanium metal is the most commonly used active element and is the active element used in both the Copper ABA and MSU synthesized braze powders. Titanium getters oxygen from the YSZ at the YSZ/braze interface, creating a reactive bond between the metal and the ceramic in the form of a titanium oxide. These titanium oxides not only aid in the formation of a strong bond, but also assist in oxidation resistance, protecting the internal structure of the metallic braze. [3]

Braze Melting Temperature

The typical operating temperature for a planar SOFC is between 700 °C and 900°C so it is important that the braze metal be able to withstand a high temperature environment. Copper ABA was selected for use as a braze metal because of its high melting temperature and lack of precious metal additives. The commercially available Copper ABA braze alloy has a solidus melting temperature of 958 °C and a liquidus melting temperature of 1024 °C, according to Wesgo Materials. [17]

Binary phase diagrams, shown in Figures 8, 9 and 10, can be used to determine the liquidus temperature for Cu-Si, Cu-Al and Cu-Ti alloys. The information obtained from the phase diagrams can be used to approximate the melting temperature of the braze

powder. The slope of the liquidus line for each binary diagram also indicates which elements most dramatically affect the melting temperature of the bulk braze.

Cu-Al

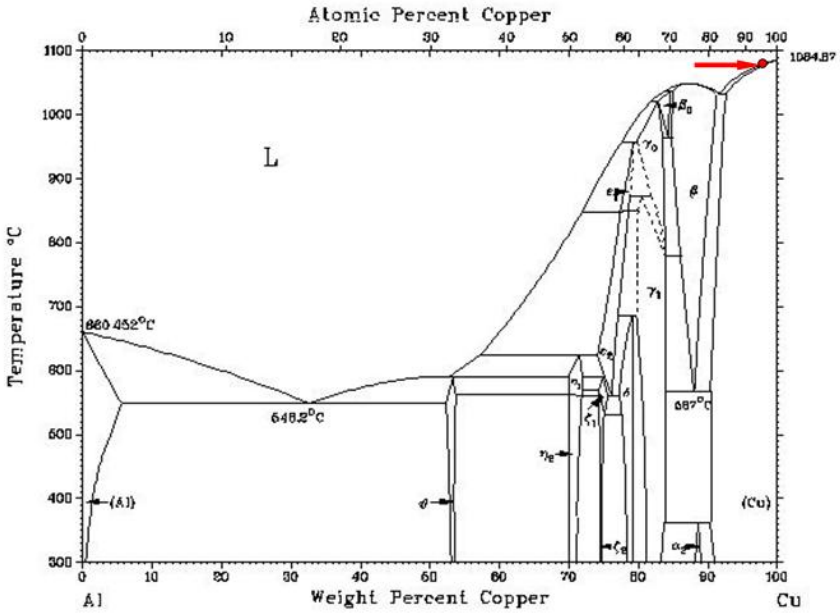

Figure 8 Cu-Al Phase Diagram Indicating Liquidus Temperature [3]

Cu-Ti

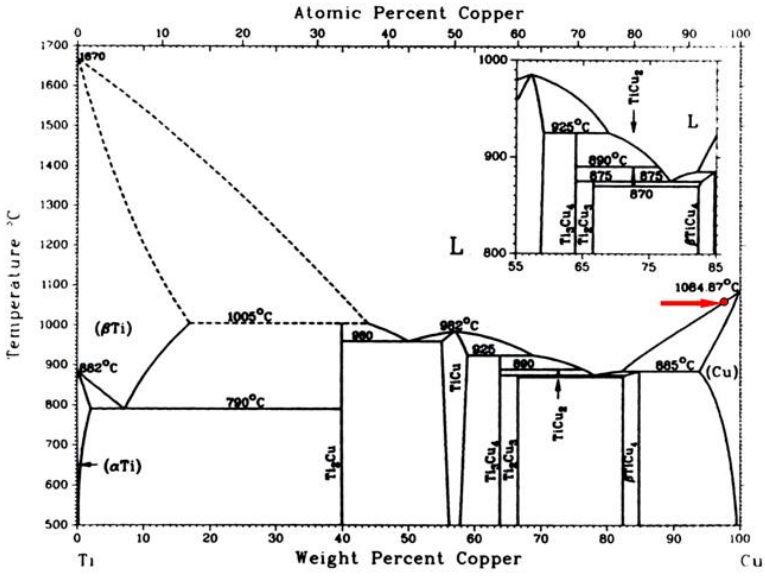

Figure 9 Cu-Ti Phase Diagram Indicating Liquidus Temperature [3]

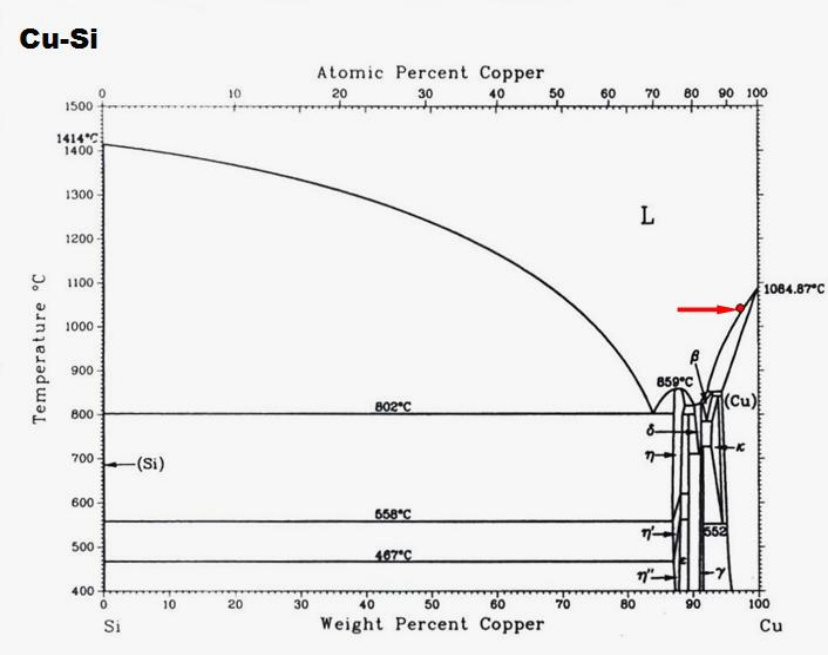

Figure 10 Cu-Si Phase Diagram Indicating Liquidus Temperature[3]

MATERIALS AND PROCEDURE

Raw Materials

The raw materials used for this study included a commercially available braze alloy (Copper ABA) as well as individual metal powders. The commercial braze was selected as a reference for braze seal research and the individual metal powders were used in the formation of custom Montana State University (MSU) synthesized brazes.

Copper ABA

The copper-based braze alloy, Copper ABA, was selected for use as the reference braze because this particular powder composition is free of high-cost precious metal additives such as silver, gold and platinum and is designed for brazing of ceramics, including YSZ. [17]

Table 2 Product Information for Copper ABA (Wesgo Materials*) [17]

Property	Copper ABA
Elemental Composition	92.75 wt% Copper
	3.00 wt% Silicon
	2.25 wt% Titanium Hydride
	2.00 wt% Aluminum
Particle Size	-325 Mesh
Solidus Temperature	958 °C
Liquidus Temperature	1024 °C
Coefficient of Thermal Expansion	19.5×10^{-6}/°C
Electrical Resistivity	$198\times10^{-9}\ /\Omega\cdot m$
Electrical Conductivity	$5.1\times10^{6}\ /\Omega\cdot m$
Density	8.1 $^{g}/_{cm^3}$
Young's Modulus	96 GPa
Yield Strength	279 MPa
Tensile Strength	520 MPa
Thermal Conductivity	38.0 $^{W}/_{m}K$

*Information provided from manufacturer

MSU Braze Materials

In-house synthesized braze powders were developed and tested at Montana State University using powder metals. With the objective of optimizing braze behavior for SOFC specific application, elemental powder mixtures were used to replicate the commercial braze, Copper ABA, and to create tailored braze compositions. All metal powders were purchased from Alfa Aesar.

Table 3 Description of Metal Powders used for In-house Synthesized Braze Powders

Element	Description
Cu	Copper Powder, -625 mesh, APS 3.25-4.75 micron, 99.9% metals basis
Si	Silicon Powder, nodular, APS 1-5 micron, 99.999% metals basis
Al	Aluminum Powder, -325 mesh, APS 7-15 micron, 99.5% metals basis
Ti	Titanium Powder, -325 mesh, 99.5% metals basis
TiH_2	Titanium (II) Hydride
Al_2TiO_5	Aluminum Titanium Oxide Powder, 99.5% metals basis

Fabrication of YSZ

YSZ disks were fabricated using 8 mol % Yttria-Stabilized Zirconia powder[18] with a nominal particle size of 0.5 microns. While the exact dimensions of the YSZ disks do not have a large effect on this study, the final diameters for the densified YSZ disks were approximately 24 mm in diameter.

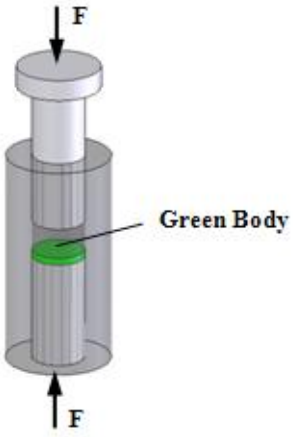

Figure 11 Dry Pressing Procedure for Fabrication of YSZ Disks [3]

Powder batches of 4.5g were placed in a 25.4mm (1inch) diameter punch and die, as represented in Figure 10, and pressed to a pressure of approximately 100 MPa. The green (un-sintered) pellets were then sintered at a temperature of 1500 °C for two hours to reach 99 % densification and no open porosity. The sintering temperature profile can be seen in Figure 12. The temperature was increased at a rate of 5 °C per minute to 1500 °C, held for two hours at 1500 °C and then cooled at a rate of 10 °C per minute.

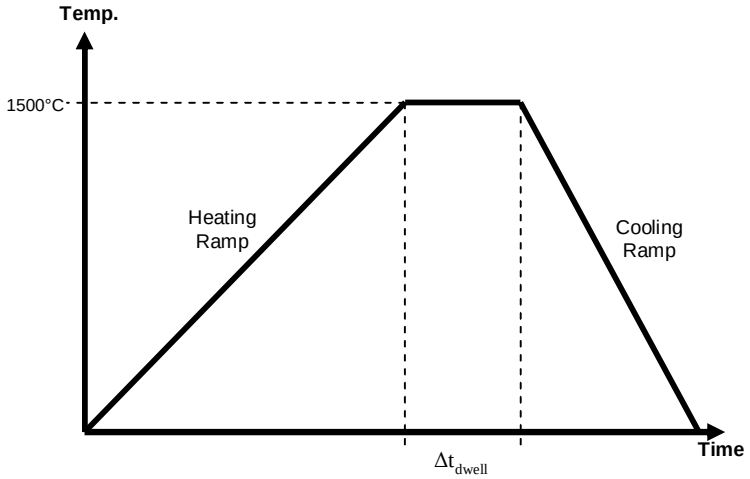

Figure 12 Temperature Profile for YSZ Sintering

Fabrication of Stainless Steel

430 stainless steel sheets were purchased (Ace Hardware, Bozeman, MT) for use in the brazing experiments to represent the interconnect material in an SOFC stack. Circular disks were laser cut from the sheets by a laser machining company (JE Soars, Belgrade, MT). Laser cutting was utilized to minimize distortion from traditional cutting and punching processes. The final stainless steel disks were approximately 25.24 mm in diameter and 0.3 mm thick.

Organic Binders

Organic binders were used in the braze pastes to prevent the braze powders from being pulled from the braze joint as the furnace chamber was being evacuated, providing mechanical stability. Polypropylene carbonate binders are clean-burning, thermally decomposable binders that break down into CO_2 and water in various types of atmospheres. The polypropylene carbonate binders are amorphous, clear thermoplastics which burnout at elevated temperature leaving virtually no residue. Residual residue in the brazing chamber can yield unreliable braze performance.

QPAC 40

QPAC 40 is an organic-based binder purchased from Empower Materials. QPAC 40 utilizes a poly(propylene carbonate) to act as the binder compound. Table 4 shows the compositional make-up for the QPAC 40 binder and Table 5 lists important material properties for the QPAC 40 binder.

Table 4 Compositional Information for QPAC 40[19]

Material	Weight Percent
Poly(propylene carbonate)	94+
Propylene Carbonate	0-5
Methylene Chloride	0.2-0.8

Table 5 QPAC 40 Material Properties Information[19]

Property	QPAC 40 (PPC) Poly(propylene carbonate)
Molecular Weight (number average)	250,000
Density ($^{g}/_{cm^3}$)	1.26
Tensile Strength (psi @ 23 °C) @yield @break	 4,500 1,760
Elongation (%) @yield @break	 3.5 150
Modulus of Elasticity (kpsi)	300
Melt flow index ($^{g}/_{10\,\min}$ @ $^{150^{\circ}C}/_{2160\,g}$)	0.9
Hardness (Shore D)	79
H2O Absorbtion @ 23 °C (5)	0.4
Loss Tangent (103 Hz)	0.007
Haze (%)	3.6
Decomposition Temperature (°C)	250
Glass Transition Temperature or T_g (°C)	40
Heat of Combustions ($^{cal}/_{gm}$)	4,266
Heat of Formation ($^{kcal}/_{mol}$)	-145.647
Molar Mass	102.1

A typical composition for a paste utilizing the QPAC 40 binder (as reported by Empower Materials) usually consists of a glass ceramic, QPAC 40, a plasticizer and a dispersant. Approximate amounts of each constituent, on a weight percent basis, are shown in Table 6.

Table 6 Compositional Recipe of a Typical Paste Utilizing QPAC 40[19]

Material	Weight Percent
Ceramic/Glass	85-90 %
QPAC 40	10-15 %
Plasticizer	3 %
Dispersant	2 %

Plasticizers and dispersants were not utilized in any of the braze paste compositions created for this research. Typical braze paste compositions consisted of approximately one weight percent QPAC 40 binder to 99 weight percent braze powder. In this manner the binder was not intended to provide any mechanical strength beyond that of holding particles together during the initial vacuum stage.

The QPAC 40 binder was dissolved in a solvent (either Methyl Ethyl Ketone (MEK) or cyclohexanone) before being added to the braze powder to ensure an even distribution of binder throughout the braze paste. Five grams of QPAC 40 binder was dissolved into 45 grams of solvent (solubility limit as reported by Empower Materials). The binder/solvent solution was then added to the braze powders in a ratio of 1.01g of binder/solvent solution for every 10 g of braze powder. The braze powder, binder/solvent solution ratio ensured that approximately one weight percent of QPAC 40 binder was present in the final braze paste after evaporation of the solvent.

QPAC 40 Emulsion

QPAC 40 Emulsion is a specialized type of the QPAC 40 binder. Emulsion allows for aqueous dispersion and can be completely dissolved in water. The compositional information for QPAC 40 Emulsion is shown in Table 7 below.

Table 7 Compositional Information for QPAC 40 Emulsion[19]

Material	Weight Percent
Poly(propylene carbonate) $(C_4H_8O_3)_8$	50-20
Propylene Carbonate	0-5
Water	45-65
Proprietary Surfactants	5-10

Mixing Procedure

A mixing process was developed for the purpose of thoroughly mixing the brazing powders and making a paste-like substance which can easily be applied to the samples. The binder/solvent solution was added to the braze powder compositions so that each braze paste contained approximately one weight percent binder. The braze slurries were then mixed into a paste using a Branson Sonifier 450 ultra sonic mixer.

The exact weight percent of binder in the braze paste can be calculated using the following equations:

$$\frac{XgQPAC40}{(XgQPAC40 + YgCyclohexanone)} = Z$$

Equation 3 Equation for Binder Concentration in Binder/Solvent Solution

$$\frac{5gQPAC40}{(5gQPAC40 + 45gCyclohexanone)} = 0.1 = 10wt\%QPAC40$$

Equation 4 Calculation for 10 wt % Binder in Binder/Solvent Solution

$$\frac{XgQPAC40}{(XgQPAC40 + YgBraze)} = 0.01$$

Equation 5 Equation for Binder Concentration in Braze Paste

$$\frac{XgQPAC40}{(XgQPAC40 + 10gBraze)} = 0.01 \qquad QPAC40 = 0.1010g$$

Equation 6 Calculation for 1 wt % Binder in Braze Paste

$$\frac{0.1010gQPAC40}{(XgQPAC40/CyclohexanoneMix)} = 0.1 \qquad QPAC40/Cyclohexanonemix = 1.010g$$

Equation 7 Calculation for Amount of Binder/Solvent Solution to obtain 1 wt % Binder

Braze pastes were prepared in 10 g batches of braze powder. Calculations using the above equations indicate that 1.01 g of binder/solvent solution should be added to a 10 g batch of powder to ensure approximately one weight percent of binder in the braze paste.

Solvent Selection

The vapor pressure of the solvent plays a critical role in the successful application of the braze paste. If the selected solvent has a high vapor pressure, then the braze paste will begin to dry before proper application of the brazing paste to the interconnecting materials has taken place. A braze paste which dries too quickly can result in poor wetting of the ceramic disk which could result in a weak bond between the metallic braze and the SOFC materials.

Table 8 lists the vapor pressures for the some of the solvents that Empower Materials lists as being capable of dissolving QPAC 40.

Table 8 Vapor Pressure and Surface Tension Information for Solvents of QPAC 40

Solvent	Chemical Formula	Vapor Pressure (mm Hg at 20 °C)	Surface Tension (dyn/cm at 20 °C)
Acetone	C_3H_6O	181.7	23.7
1,2-DiChloroethane	$C_2H_4Cl_2$	64	38.75
Trichloroethylene	C_2HCl_3	57.8	25.4
Chloroform	$CHCl_3$	159	27.2
Ethyl Acetate	$C_4H_8O_2$	86	23.75
Methyl Ethyl Ketone	C_4H_8O	77.5	24.6
Cyclohexane	C_6H_{12}	77	24.98
Tetrahydrofuran	C_4H_8O	143	26.4
Ether Acetate	$C_4H_8O_2$	3.7	23.75
Benzene	C_6H_6	74.6	28.88
Cyclohexanone	$C_6H_{10}O$	2	42.7

Braze Joining Atmosphere

An oxygen free atmosphere must be used during the high temperature braze procedure in order to avoid oxidation and obtain a strong, hermetic bond between the metallic braze and the components of the SOFC. Residual oxygen in the heating chamber during the joining procedure can cause non-metallic layers to form on at the braze interface leading to a poor bond. Additionally, residual oxygen at elevated temperatures can lead to oxidation of the adjoining materials, such as the stainless steel. Therefore, brazes are often done in vacuum or inert gas environments such as: argon, helium, hydrogen or a mixture of the aforementioned gases.

Two inert environments were utilized for this research. A majority of the brazing tests were conducted in a mid-level vacuum environment (approximately 10^{-4} to 10^{-5}

mbar). Additional brazing tests were carried out in an inert Argon environment in which Argon was purged through the furnace system and then Argon pressure was held between ½-1 psi for the brazing process.

The brazing process was conducted using the R.D. Webb Red Devil Vacuum Furnace #80.

Figure 13 R.D. Webb Red Devil Vacuum Furnace

Braze Temperature Cycles

Samples were brazed at approximately 10-15 °C above the liquidus melting temperature of the Copper ABA braze. The temperature in the brazing furnace was increased at a relatively slow rate of 2 °C per minute to ensure that the brazing components were in a perpetual state of vacuum during the brazing process. In addition to the slow temperature ramp rate, two temperature dwells were introduced during the ramp in the furnace temperature. The furnace temperature was held at 200 °C for 15 minutes, slowly increased and then held again at 400 °C for an additional 15 minutes to

ensure that residual moisture from the binder/solvent solution and trapped moisture in the furnace insulation were being sufficiently removed from the system. The dwells at 200°C and 400 °C were selected because QPAC40 decomposes at approximately 250 °C (Table 5). The 200 °C dwell ensured the burnout of residual moisture from water in the air (water evaporates at 100 °C) and the 400 °C dwell ensured that there was ample time for the binder to decompose completely. This process helped to ensure that the furnace chamber was in a continuous state of mid-level vacuum. The brazing temperature profile can be seen in Figure 14.

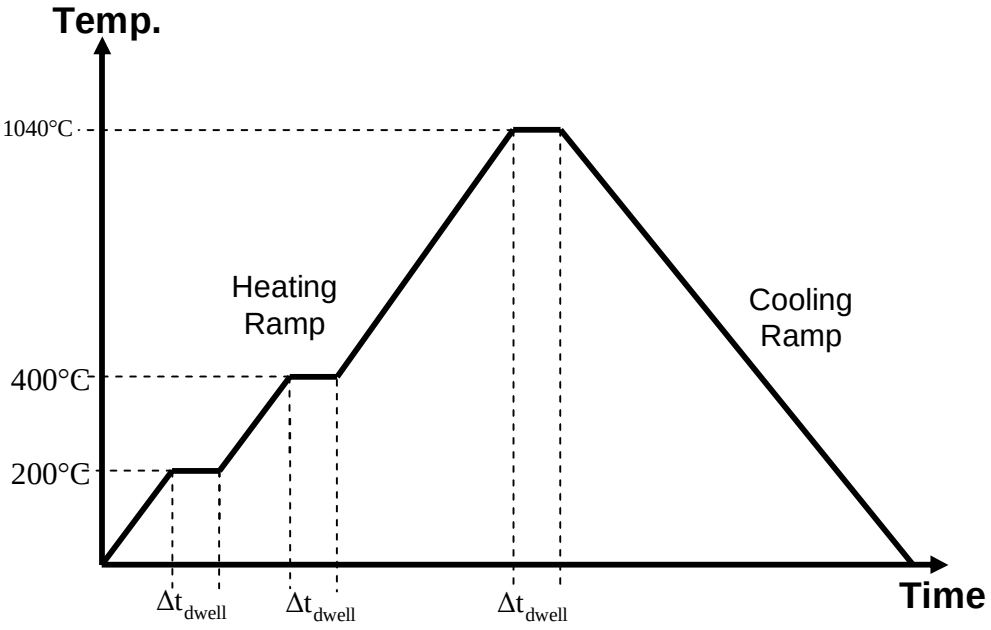

Figure 14 Temperature Profile for Brazing Process

Cross-Sectioning and Polishing

After a successful braze joint has been achieved, braze samples were then cross-sectioned using a diamond saw (Isomet 1000, Buehler Corp.). The cross sectioned

samples were mounted in a rigid epoxy to ensure a stable environment which would allow for polishing of the samples utilizing a rotary semi-automatic polisher (Euromet 4, Buehler Corp. Lake Bluff, Illinois). Polishing was performed using silicon carbide abrasive papers and finished with a 0.5 micron alumina compound on a billiard cloth wheel.

Pelco fast curing epoxy (Ted Pella, Inc.) was used to mount the samples. The epoxy utilized a ratio of two parts epoxy to one part rigidizer. Samples were placed in a small plastic mounting dish, cross-sectioned side down. Mixed epoxy was poured over the cross-sectioned sample and the dish of epoxy was placed in a drying oven overnight while the epoxy cured. After the epoxy was hardened, the surface of the epoxy exposing the cross-sectioned sample was polished on an electric sand disk with a final polishing on a disk of 0.5 microns, allowing the sample to be clearly seen by the naked eye. The clean surface was analyzed using Field Emission Microscopy.

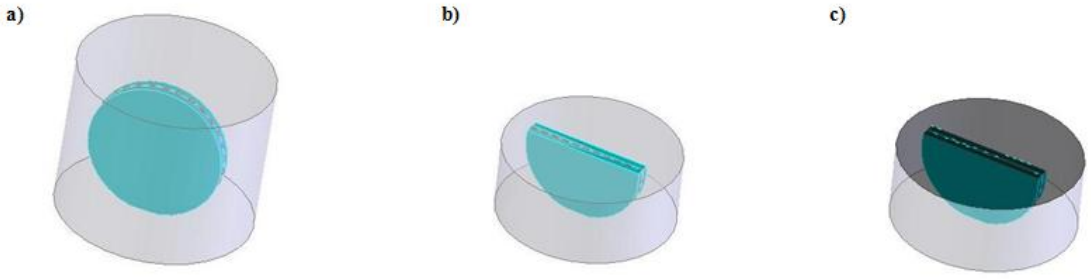

Figure 15 Cutting and Mounting of Braze Sample for Image Analysis [3]

FEM and EDS Analysis

Braze interface microstructure was characterized by Field Emission Scanning Electron Microscopy (FEM) and Energy Dispersive X-ray Analysis (EDS) using the Zeiss Supra 55VP, Carl Seiss NTS GmbH Field Emission Microscope.

The surface of the polished, epoxy mounted samples were painted with a Colloidal Graphite (Ted Pella, Inc. SG=0.89) to aid in the reduction of charging during the imaging process. The samples were then sputter-coated with a thin film of carbon using a peltier cooled sputter coater (EMITECH K575X). The thin film of carbon acts as an electrically conductive surface which also aids in the reduction of charged particles in the chamber of the FEM, allowing for clearer microscopic imaging. The application of colloidal graphite in addition to sputtering improves the conductivity for EDS analysis to be performed at the necessary high accelerating voltages.

Pop-Gun Testing

Pressurized rupture tests were conducted on specialized brazed joints to characterize bond strength and determine the formation of a hermetic seal. Pressure test rupture cups (see Figure 16) were machined out of a 25.4 mm (1 inch) diameter, 440 stainless steel rod. The rupture cups included a flat top surface which allowed for brazing to a small YSZ disk. The bottom of the rupture cup was machined with a ¼ NPT thread to allow the final brazed cup to be attached to an Omegadyne pressure transducer (Model: PX209-300G5V, S/N: 47425).

The 440 stainless steel pressure test piece and YSZ disks were first cleaned in an ethanol bath for approximately five minutes. Braze pastes were then extruded onto the ringed portion of the pressure test rig using a paste extruder. The YSZ disks were quickly placed atop the pressure test cup and additional braze was applied around the edge of the YSZ disk to help obtain a hermetic seal between the rupture cup and the YSZ disk. The samples were then dried in a drying oven for approximately 30 minutes. The samples were placed YSZ side down in the braze furnace, allowing the weight of the 440 stainless steel test cup to keep pressure on the braze ring at all times during the brazing process. Samples were brazed in a mid-level vacuum environment (approximately 10^{-4} to 10^{-5} mbar) under the temperature profile shown in Figure 14.

Figure 16 440 Stainless Steel Machined Rupture Cup

After the braze furnace had cooled, the pressure test samples were removed from the furnace and connected to a pressure test rig which allowed for the small internal region beneath the YSZ disk and braze region to be pressurized (see Figure 16). Rupture

samples were slowly filled with Argon gas, increasing pressure in the internal region until fracture occurred and all pressure was released. Pressure measurements were recorded every $\frac{1}{10}$ of a second using a software package from Agilent Technology.

Samples were tested to a maximum pressure of 150 psi, the maximum rated pressure of the bottle regulator. Samples that reached a pressure of 150 psi without fracturing were then evaluated for the formation of a hermetic seal. To inspect for a hermetic seal, the pressure in the internal chamber of the sample were reduced to between 30 to 50 psi and the regulator valve closed to ascertain the extent of seal leakage. A data acquisition system would measure the chamber pressure every $\frac{1}{10}$ of a second to register any decrease in pressure in the internal region of the test sample, indicating a leak in the seal. All tests were conducted at room temperature.

Figure 17 Experimental Set-up for Pressurized Rupture Test

Differential Thermal Analysis

Differential Thermal Analysis (DTA) measures the temperature change of a sample relative to the temperature of a non-reactive reference sample as the DTA chamber is heated. The temperature difference between the sample and the reference is measured by two thermocouples placed beneath the samples, as indicated by Figure 18. The measured temperature differences determine endothermic (heat absorbed) or exothermic (heat released) reactions which are used to investigate thermal properties and phase changes of the samples which may be unknown. The endothermic and exothermic peaks detected with DTA give an indication of the solidus and liquidus melting and solidification temperatures for the braze powders. [20]

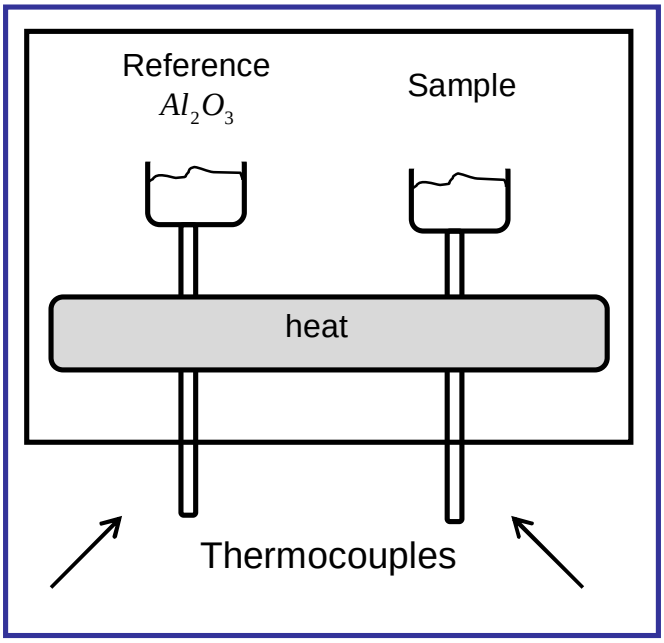

Figure 18 Schematic for DTA Analysis

As a material is heated, elemental bonds begin to break, the energy required to break these bonds is obtained through heat absorption. The absorption of heat is an indication that the material has begun the melting process. Conversely, as a material is cooled from its liquid state, energy is released during bond formation; this release in energy indicates the solidification of the material. The DTA system is able to record these peaks in temperature change giving an indication of the solidus and liquidus melting and solidification temperatures of the material being analyzed.

Figure 19 shows an example DTA curve for the Copper ABA braze powder. Arrows have been used to indicate the heating curve and the cooling curve. An upward DTA peak indicates an endothermic reaction in which heat is absorbed and a downward pointing peak indicates an exothermic reaction in which heat is released.

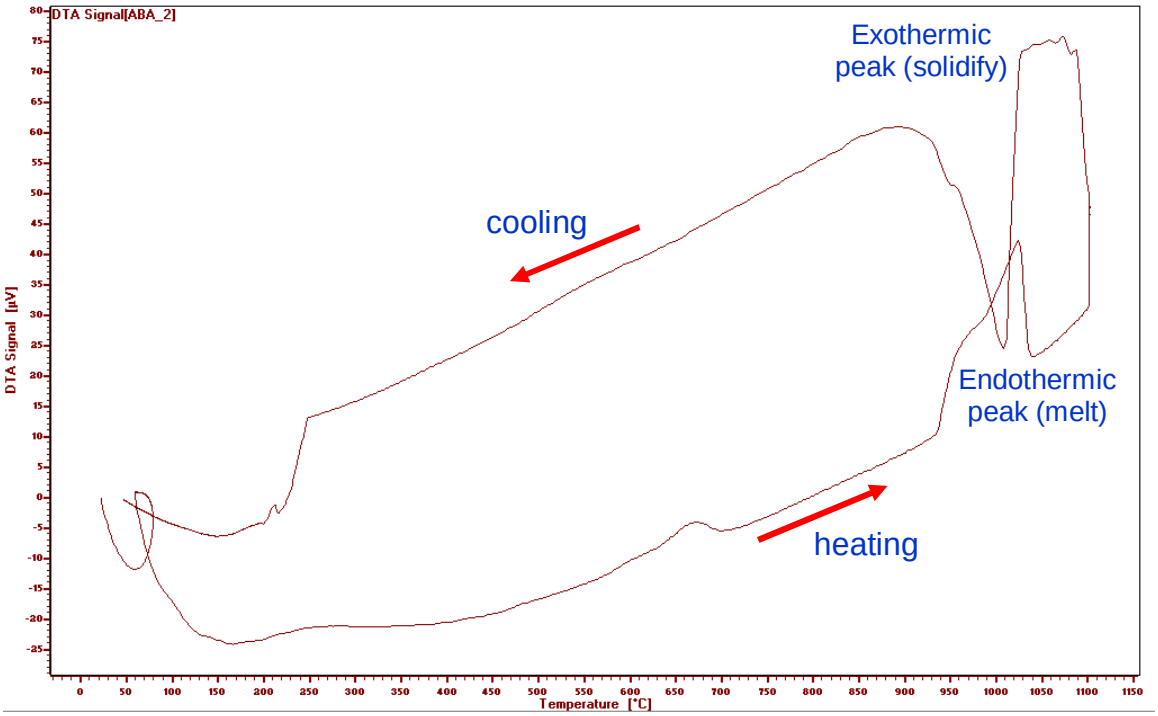

Figure 19 Typical DTA Heating and Cooling Curve

The y-axis in the DTA curve is output in μV due to the fact that a thermocouples output reading is in μV. Since the DTA curve is recording the difference in temperature from the reference sample to that of the sample being tested, it is not necessary to convert this value to a measure of temperature. Additionally, it can be seen that the cooling curve and the heating curve are not registering temperature difference. This could be due to the fact that as the sample melted, the particles of the material have moved and taken on a new shape, the material may have also changed in weight slightly. Both of these processes could alter the temperature difference registered by the thermocouple. This phenomenon does not affect the quality of the DTA results of interest for this research.

Thermal Gravimetric Analysis

Thermal Gravimetric Analysis (TGA) measures the relative change in mass of a sample to that of a non-reactive reference sample as a function of increasing temperature. TGA utilizes that same internal chamber set-up as the DTA, which is shown in Figure 18. The samples in the TGA are balanced on an arm. A linear actuator is used to measure the change in position of the arm as a result of mass change in the sample during thermal treatment, unbalancing the scale. TGA can give an indication to the oxidation behavior of a material by recording the relative weight loss or gain of a sample to that of the reference as a function of time.

An example of a TGA curve is shown in Figure 20. The figure shows a material that has gained mass over time in a thermally treated environment. A linear TGA curve would suggest that the material being analyzed oxidizes at the same rate regardless of

time. The parabolic shape of the TGA curve shown in Figure 20 indicates that the material being analyzed has formed a diffusion limited oxide scale, suggesting that the material has formed a barrier, creating an impermeable path to oxygen. After the material has formed this initial oxide scale, the material is no longer able to oxidize. With the material protected from further oxidation, the internal structure of the material remains intact and protected, maintaining the strength characteristics of the material in the internal, un-oxidized region.

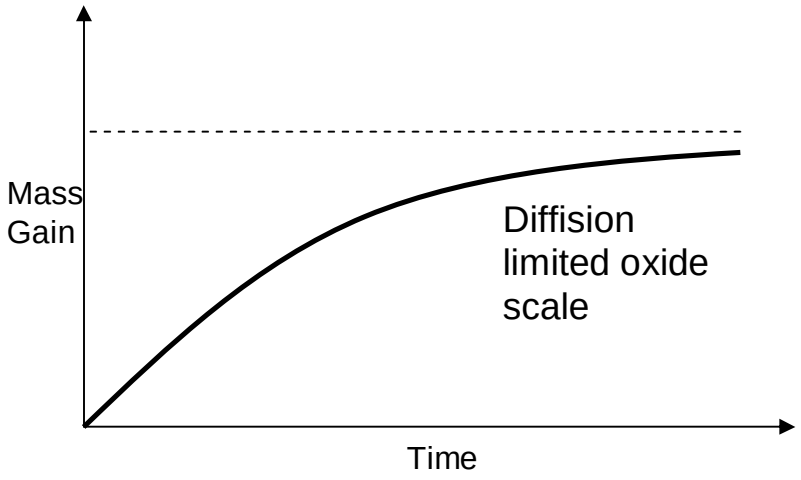

Figure 20 Example TGA Curve Indicating Diffusion Limited Oxide Barrier

TERRA Thermodynamic Analysis Software

TERRA is a thermodynamic simulation program which identifies the possible thermodynamic reactions that can occur between materials under conditions such as change in oxygen partial pressure or temperature. TERRA was used to obtain information about the oxidation behavior of materials within the brazing powder, as well

as possible reactions that can occur between the elements which make up the braze composition.

TERRA Analysis was done for the braze compositions assuming a temperature of 800 °C and a range of oxygen content from 0.1 to 100 percent, units in $^{mols}/_{kg}$.

RESULTS AND DISCUSSION

Organics and Binder Solvent Selection

The QPAC 40 Emulsion binder was discontinued from use in the brazing experiments. The binder/solvent solution of QPAC 40 Emulsion and de-ionized water did not mix well with the braze powders, often leaving the braze powders settling to the bottom while the solvent solution remained suspended on top. When the braze paste was placed on top of the YSZ disk, the de-ionized water would separate very quickly leaving an almost dry powder on the ceramic surface, inhibiting proper wetting of the substrate.

The final binder/solvent solution selected for the braze paste compositions consisted of QPAC 40 dissolved in cyclohexanone. QPAC 40 was selected as the brazing binder as it is organic, clean burning and disperses well when mixed with the proper solvent. QPAC 40 also offered the most flexibility during experimental set-up as well as the best results during brazing tests.

Methyl Ethyl Ketone (MEK) was the first chemical selected for use as the solvent for the QPAC 40 binder. However, braze applications utilizing this solvent were difficult as the braze paste was drying too quickly for proper braze application. Cyclohexanone was selected as the final solvent as it has a very low vapor pressure (Table 8), and was easily accessible. Practice applications using the cyclohexanone solvent proved that the solvent allowed amble time for proper braze paste application.

The binder/solvent solution contains 10 weight percent QPAC 40 binder. After the solvent is completely dissolved in the binder, the binder/solvent solution is then added to the brazing powder. The brazing paste was designed to contain approximately one

weight percent binder. A ratio of 1.01 grams of the binder/solvent solution is added to every 10 grams of braze powder to obtain the desired amount of binder in the brazing paste.

Copper ABA

Figure 21 shows a brazing joint that has been pulled apart between the ceramics and stainless steel disks. The fracture pattern of the braze joint shows that fracture has occurred throughout the YSZ disk indicating a strong chemical bond between the metallic braze and the YSZ interface.

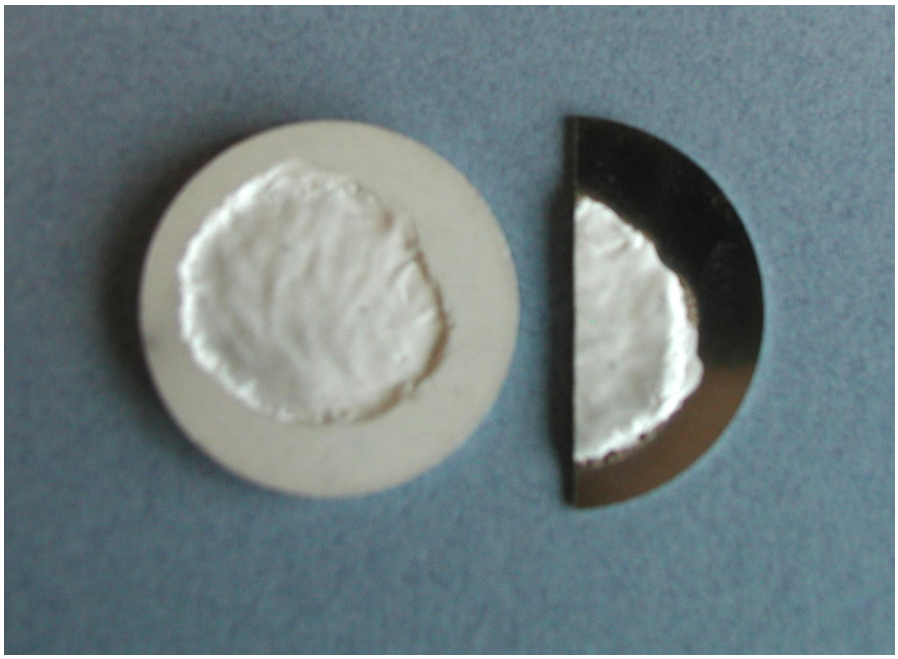

Figure 21 Copper ABA Vacuum Braze Joint

FEM and EDS Data

FEM was used to examine the micro-structural and compositional behavior at the interface between the metallic braze and the ceramic as well as between the metallic

braze and the stainless steel. EDS line scans were performed to obtained qualitative information regarding the distribution of each individual element within the metallic brazes to better understand the bonding mechanisms of the brazing material.

Vacuum Tests: Figure 22 shows an EDS line scan of a cross-sectioned YSZ disk joined to a 430 stainless steel disk with the commercial Copper ABA braze paste.

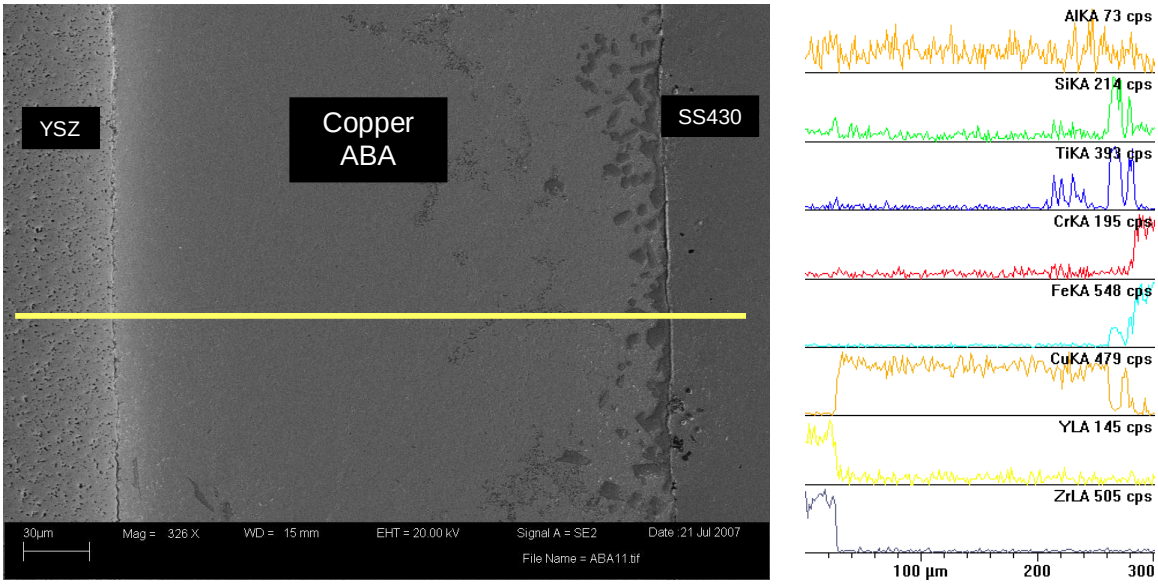

Figure 22 EDS Line-scan of Copper ABA Vacuum Braze Joint

EDS detected peaks of aluminum, silicon and titanium at both the braze/stainless steel interface as well as the YSZ/braze interface, which can be seen in Figure 23 and Figure 24, respectively. The titanium, aluminum and silicon elemental peaks indicate that a chemical bond has taken place during the brazing process. The smaller peak sizes at the YSZ/braze interface may indicate a weaker bond than at the braze/stainless steel interface. The titanium peak indicated at the YSZ/braze interface suggests that titanium is migrating to the ceramic surface during brazing, reacting with the oxygen in the YSZ to form a titanium oxide reactive layer. This metallic oxide layer could be a graded layer

of various titanium oxides such as TiO, TiO_2 and Ti_2O_3, forming a graded seal at the interface.

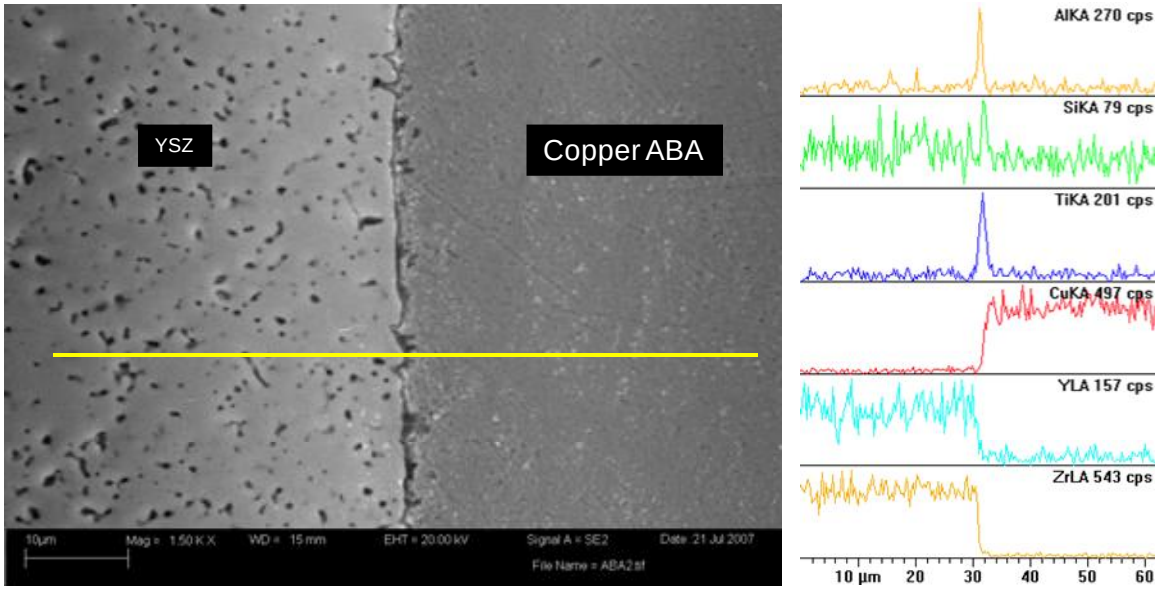

Figure 23 EDS Line-scan of YSZ/Braze Joint Interface for Copper ABA

The clusters which appear at the stainless steel/braze interface of the Copper ABA, shown in Figure 24, appear to be concentrated areas of titanium and silicon possibly in the form of titanium silicide (TiSi). The formation of this possible inter-metallic alloy could suggest an excess of titanium in the braze composition. This observation suggests a direction to develop an MSU-tailored braze composition in which the amount of titanium in the braze powder is reduced.

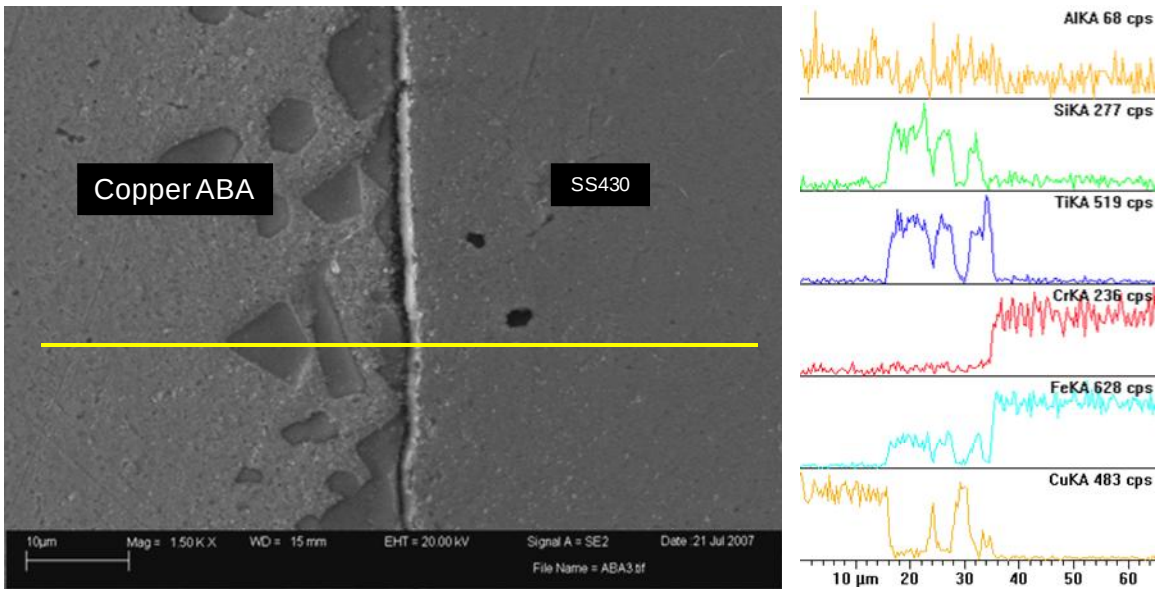

Figure 24 EDS Line-scan of Braze/SS Joint Interface for Copper ABA

Figure 25 is the edge of a portion of a braze joint brazed using the Copper ABA powder. EDS line scan indicates aluminum and titanium rich regions at the very outer edge of the joint.

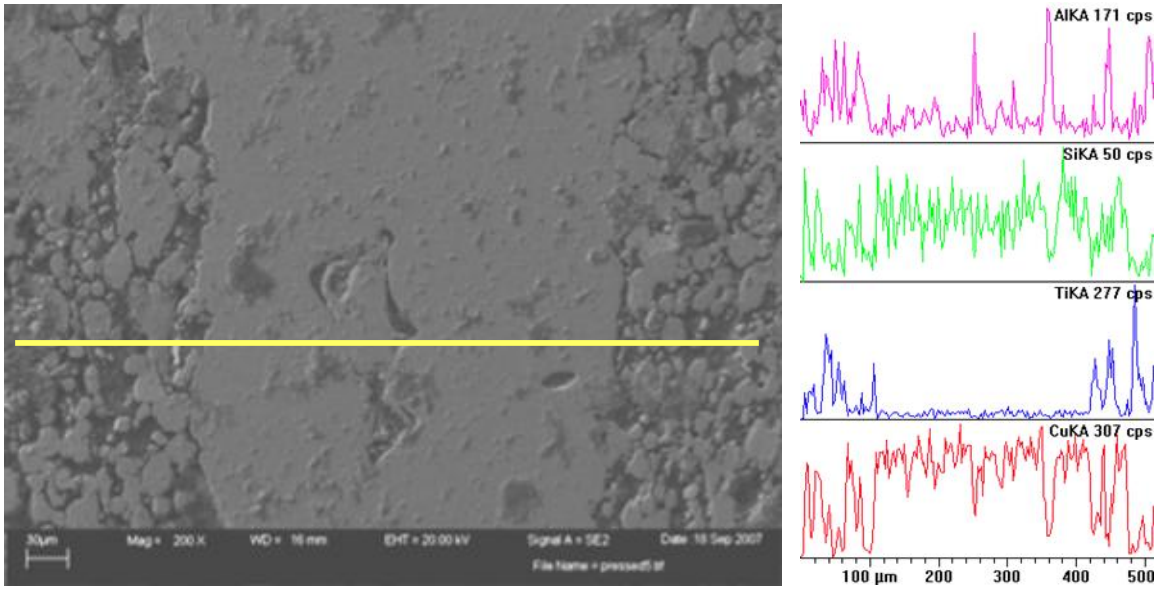

Figure 25 Indication of Ti and Al Rich Regions of Braze Edge

Due to the fact that both aluminum and titanium have a high affinity for oxygen, the titanium and aluminum may be migrating to the braze edge to getter the remaining oxygen in the braze chamber thus forming TiO_2 and Al_2O_3 barriers. The free energy of formation for these and other brazing metal oxides are shown in Table 9. The more negative the value for the free energy of formation means that the metal oxide is more stable. As shown, Al_2O_3 is the most stable metal oxide in the braze composition, followed by TiO_2.

Table 9 Free Energy of Formation for Brazing Metallic Oxides [21]

Element	Common Oxide	Free Energy of Formation at 25°C, kJ/mol
Gold	Au_2O_3	+50
Silver	Ag_2O	-10
Copper	CuO Cu_2O	-250 -300
Nickel	NiO	-430
Iron	FeO Fe_2O_3 Fe_3O_4	-490 -500 -510
Tin	SnO SnO_2	-510 -515
Zinc	ZnO	-625
Chromium	Cr_2O_3	-700
Silicon	SiO_2	-860
Titanium	TiO_2	-900
Aluminum	Al_2O_3	-1050
Magnesium	MgO	-1140

The aluminum and titanium oxide barriers will not only act to protect the internal structure of the metallic braze from oxidation, but will also locally shut off electrical

conductivity of the metallic seal, thus reducing the potential for the braze joint to hinder the electrical performance of the SOFC.

Figure 26 shows the FEM image of a Copper ABA braze joint with a large crack through the YSZ disk. This crack may have occurred due to thermal stresses imposed during the brazing process as a result of the CTE mismatch between the braze joint and the adjoining materials. The CTE for YSZ, stainless steel and the Copper ABA braze alloy were indicated previously in Table 1 along with the CTE's for the powders used in the formation of the MSU braze. The CTE for the Copper ABA braze powder is much higher than that of the adjoining materials which can introduce stresses into the SOFC materials during thermal treatment, causing small cracks to form, as is evident in Figure 26. Cracks in the electrolyte of the YSZ can cause rapid decline in the overall performance of the SOFC.

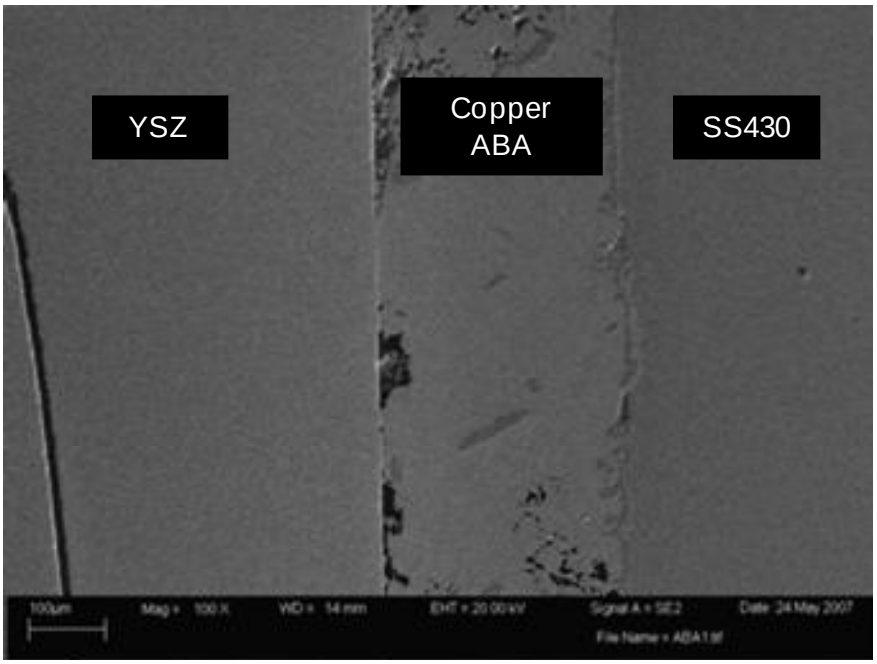

Figure 26 Fracture of YSZ due to CTE Mismatch

Argon Tests: Brazing tests conducted in an Argon gas environment did not perform as well as brazing tests conducted in a vacuum environment. Figure 27 shows a braze joint that has been pulled apart between the YSZ and stainless steel disks. Fracture of the joint has occurred mostly between the YSZ/braze interface. Some portions of the YSZ have remained attached to the braze interface, indicating partial bonding, however, not the full bonding as shown with the vacuum braze samples.

Figure 27 Fracture Pattern of Copper ABA Argon Braze Joint

EDS line-scans of Copper ABA brazing joints brazed in both vacuum and Argon has detected an increase in the amount of silicon present in the YSZ substrate after the brazing process. Silicon diffusion has been noticed to a depth exceeding 40 microns, though additional EDS line scans are necessary to determine a more accurate depth of silicon diffusion. Figure 28 shows a braze joint where the diffusion of silicon into the YSZ ceramic is significantly noticeable.

SOFC stacks are designed for long-life applications and the presence of silicon in the fuel cell can significantly hinder the life and the performance of the cell. The presence of silicon in the electrolyte of the cell is believed to lead to fuel cell degradation. "Siliceous impurities, which are very often found on YSZ surfaces after high-temperature processing, seem to increase the polarization resistance by blocking the transfer of oxygen between the atmosphere and the electrolyte." [22] The poisoning effect of silicon in the electrolyte of the cell decreases both electronic and ionic conductivity. [23] Impurities in the YSZ can segregate to the surfaces and grain boundaries of the ceramic during high temperature processing, negatively affecting the mechanical and electrical properties of the YSZ. While silicon poisoning is identified to be a problem, the amount of silicon present in a fuel cell that will negatively impact cell performance is not known at this time. [13]

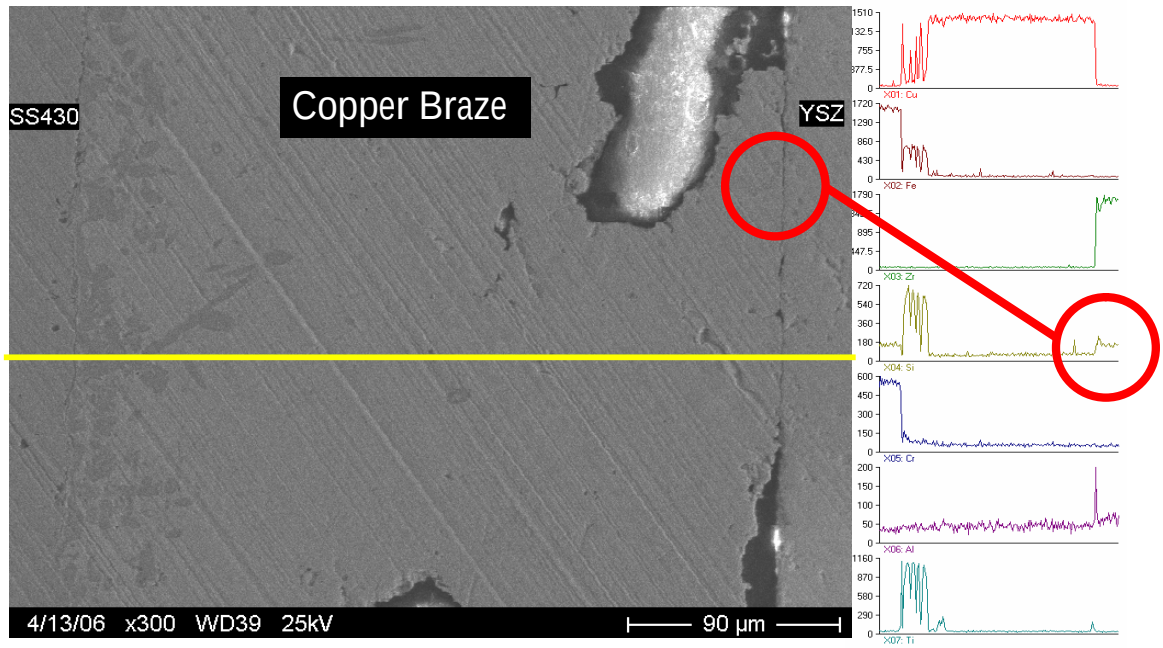

Figure 28 Copper ABA Argon Braze Joint Indicating Si Diffusion [3]

A silicon additive in copper-based alloys is done primarily for additional strength benefits as well as lowering the melting temperature of the alloy. Current copper-based alloys, such as silicon bronzes or silicon brass are examples of a copper-based alloy that exhibits low melting temperature and high strength.[24] The mechanical benefits of silicon, such as increases in yield and tensile strength are not substantial enough to be a factor for use in the application of SOFC brazing. The silicon may also act as a diffusion barrier, reacting with oxygen to form silicon dioxide. The purpose for the silicon in the Copper ABA braze alloy is not entirely understood at this time;[23] however, the slope of the liquidus curve in the Cu-Si phase diagram suggests that silicon can dramatically lower the liquidus temperature of the braze.

The deleterious effects of silicon in SOFCs in addition to the results that suggest silicon does not facilitate bonding, oxidation resistance, or improved mechanical properties yields a key application sensitive focus to remove silicon from the braze compound.

Pop-Gun Tests

Figure 29 displays a successful rupture test sample cup before rupture testing has occurred. The sample was brazed with the Copper ABA commercial braze alloy.

Figure 29 Rupture Test Sample for Copper ABA Vacuum Braze

The first series of pressurized rupture tests were conducted at room temperature on samples brazed with the Copper ABA commercial braze powder. Figure 30 shows the results of a pressurized rupture test conducted at room temperature for the Copper ABA metallic braze joint. It can be seen that the Copper ABA braze was able to withstand pressures of up to 150 psi, well above the strength needed to SOFC applications.

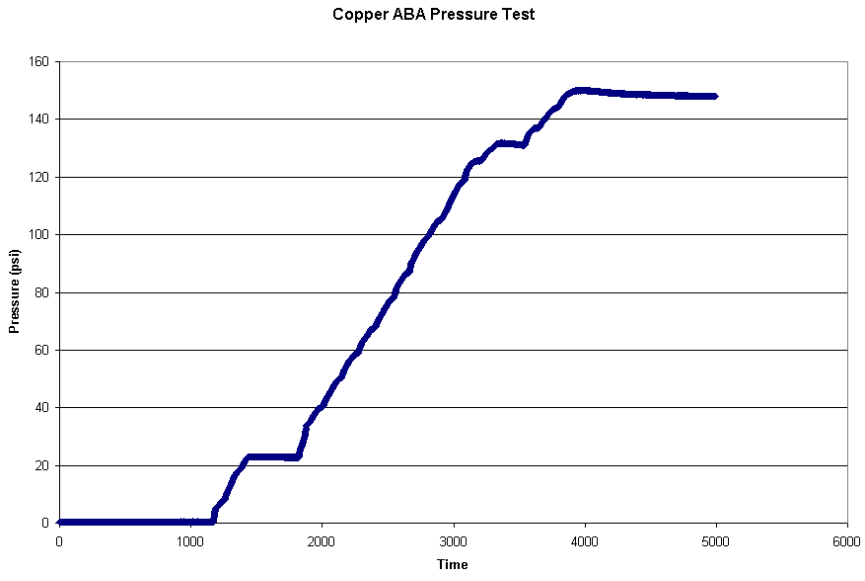

Figure 30 Pressurized Rupture Test Results for Copper ABA

The formation of a hermetic seal was obtained with the Copper ABA braze. Figure 31 shows the results of a hermeticity test in which the Copper ABA braze held a pressure of approximately 30 psi for 120 minutes, with Argon flow shut off.

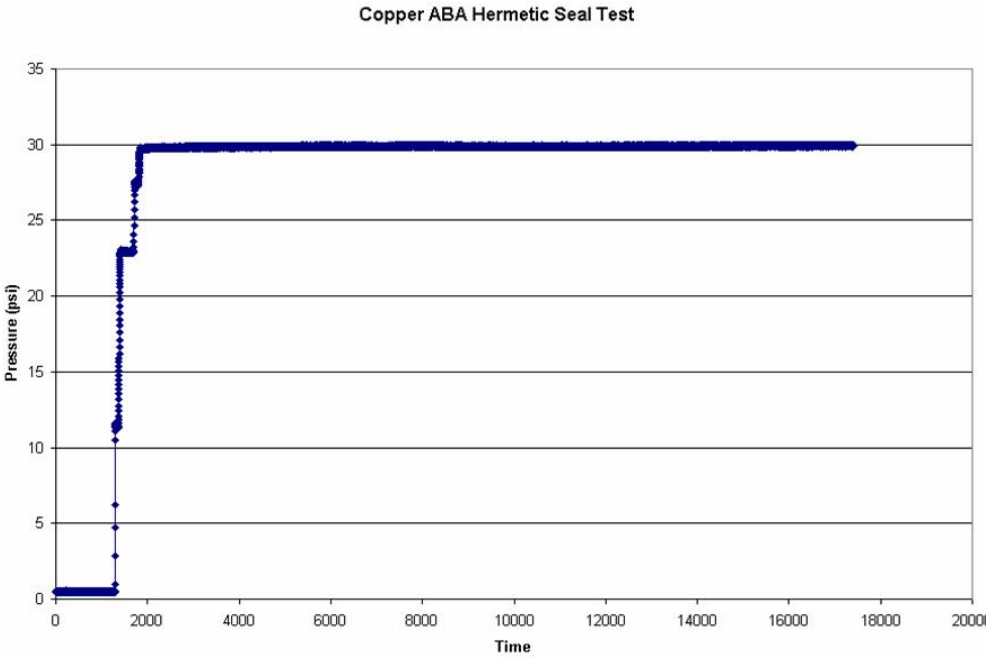

Figure 31 Copper ABA Hermetic Seal Test at Room Temperature

DTA Analysis

A DTA study was conducted in forming gas (5% hydrogen, balance nitrogen) to a temperature of 1100 °C for the Copper ABA braze powder. The braze powder was subjected to an increase in temperature at a rate of 10°C per minute up to 1100°C, the temperature was then held at 1100°C for 15 minutes and then cooled at a rate of 20°C per minute to room temperature.

The DTA results, shown in Figure 32, indicate an endothermic peak occurring at approximately 672.1°C. This peak could suggest hydrogen desorption as a result of the titanium hydride present in the Copper ABA braze powder. According to a study on the

thermal decomposition behavior of titanium hydride, TGA analysis results indicate noticeable weight-loss in Titanium-hydride at temperatures around 450-500 °C with weight-loss continuing past temperatures of 800 °C. [25]

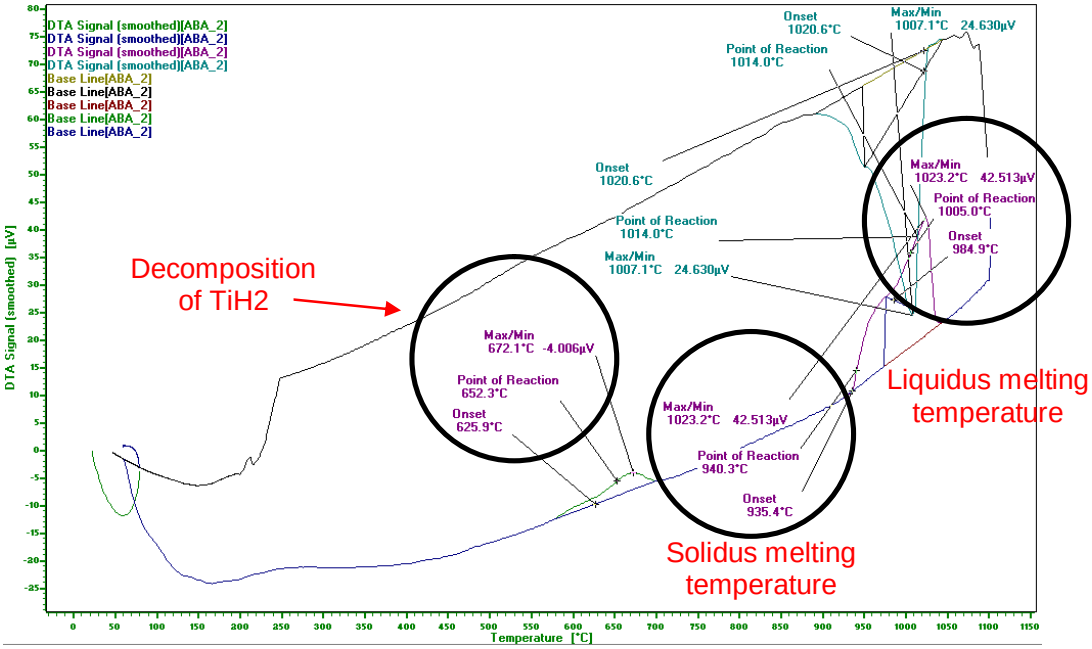

Figure 32 DTA Results for Copper ABA in Forming Gas

DTA results indicate a second endothermic peak occurring between 935°C and 1023.2°C. This peak indicates the solidus and liquidus melting temperatures of the Copper ABA braze powder. These results correspond well to the melting temperatures reported by Wesgo Materials, citing a solidus melting temperature of 958°C and a liquidus melting temperature of 1024°C.

An exothermic peak is indicated at approximately 1007.1°C. This peak corresponds with the re-solidification of the braze melt. The melting and solidification points of the peaks do not typically correspond to the same temperature due to the fact

that melting can occur homogeneously, however, crystallization can be suppressed by rapid cooling and lack of good heterogeneous nucleation sites.

TGA Analysis

A TGA study was conducted on the Copper ABA braze powder. The braze powder was subjected to a temperature increase to 850 °C and then held constant at 850°C for six hours and 25 minutes in flowing air.

The TGA results shown in Figure 33 indicate the oxidation behavior for the Copper ABA brazing powder. The parabolic shape of the TGA curve suggests that the Copper ABA braze forms a diffusion limited oxide barrier, a scale which has formed on the outside of the brazing powder, keeping additional oxygen from penetrating the interior of the braze. The scale that has formed is likely an aluminum or titanium oxide in the form of Al_2O_3, or TiO. The silicon in the braze powder could be aiding in the oxide barrier in the form of a SiO_2 scale.

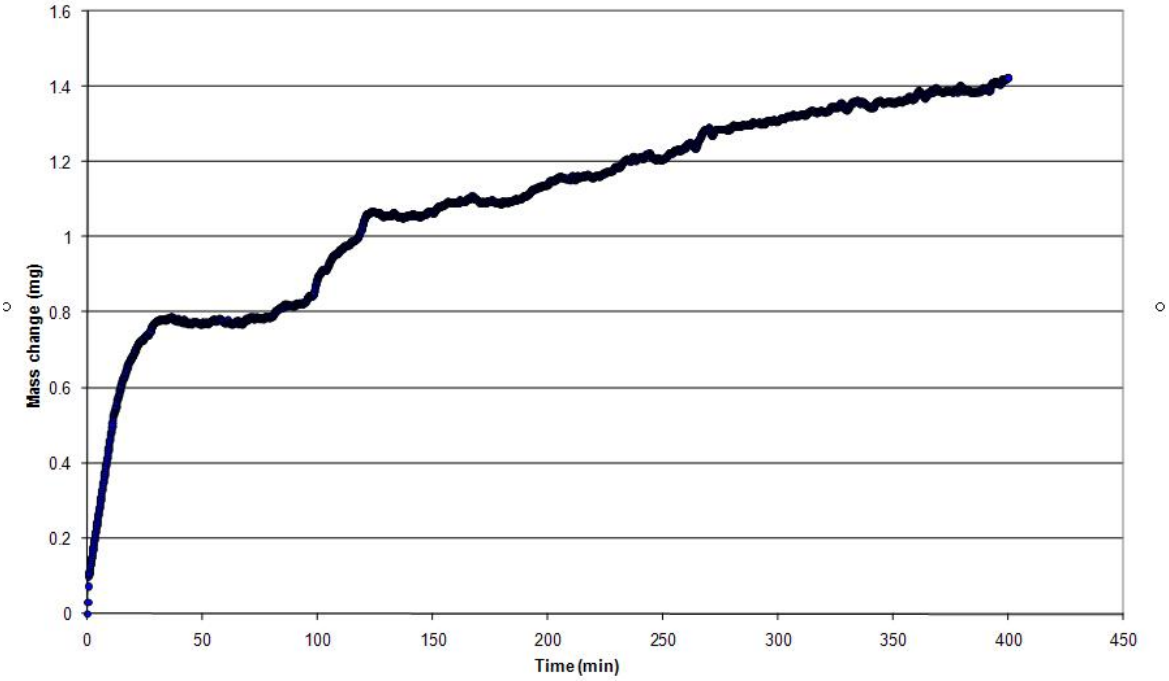

Figure 33 TGA Analysis of Copper ABA in Air

The rate of oxidation at room temperature is a generally slow process for most metals. However, at elevated temperatures, the oxidation rate increases severely, which can be problematic in many engineering applications. When a metal is exposed to air, a thin film called an oxide will begin to form. For oxidation to continue further, oxygen must penetrate the thin film oxide.

Oxidation rates of metals are determined by monitoring the weight gain of a material as it is exposed to oxygen over time. If the metal yields a linear weight gain over time, the metal is oxidizing at a constant rate and can be calculated using the following equation:

$$\frac{dm}{dt} = k_l \qquad \text{giving} \qquad \Delta m = k_l \times t$$

Equation 8 Rate of Linear Oxidation [26]

where k_l is the linear kinetic constant. Linear oxidation is the result of the oxide film cracking, allowing additional oxygen to penetrate the interior of the metal, until the entire component has been oxidized.

If the metal yields a weight gain in which the rate of the weight gain decreases with time, then the metal oxidizes in a parabolic fashion. This is due to the original oxide layer forming a compact layer, which acts as a barrier to oxygen, thus protecting the internal structure of the metal. An oxidation rate of this type can be calculated using the following equation:

$$\frac{d(\Delta m)}{dt} = \frac{k_p}{\Delta m} \qquad \text{giving} \qquad \Delta m^2 = k_p \times t$$

Equation 9 Rate of Parabolic Oxidation [26]

where k_p is the parabolic kinetic constant. [26]

TERRA

Figure 34 is a plot depicting the possible reactions occurring between the YSZ and the braze metal as a function of oxygen partial pressure. This figure indicates the formation of an aluminum oxide followed by the formation of silicon and titanium oxides, respectively. The aluminum oxide is believed to form a diffusion limited oxide barrier, protecting the internal structure of the braze, while the titanium oxide creates the chemical bond between the metallic braze joint and adjoining SOFC materials. The primary function of the silicon oxide is not entirely understood.

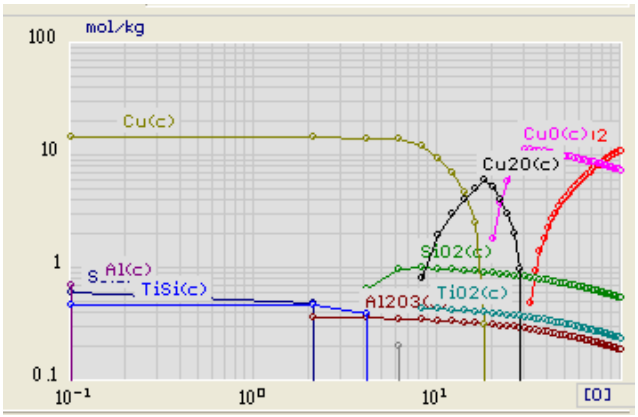

Figure 34 TERRA Analysis for Copper ABA Braze Elements

TERRA also indicates the possibility of the formation of certain inter-metallic alloys such as TiSi. This result corresponds with EDS images, such as Figure 21 which indicates TiSi clusters within the internal structure of the braze material.

Figure 35 is a second TERRA plot for Copper ABA showing additional inter-metallic alloys which may be forming within the metallic braze joint. $ZrAl_2$ and ZrSi are indicated to form at large oxygen partial pressures. EDS line scans have indicated peaks of aluminum and silicon at the YSZ/braze interface, these peaks could be the result of the possible formation of the aforementioned inter-metallic alloy. This result also indicates that aluminum and silicon may aid in the chemical bonding between the ceramic and the braze metal by bonding with the zirconium in the YSZ disks.

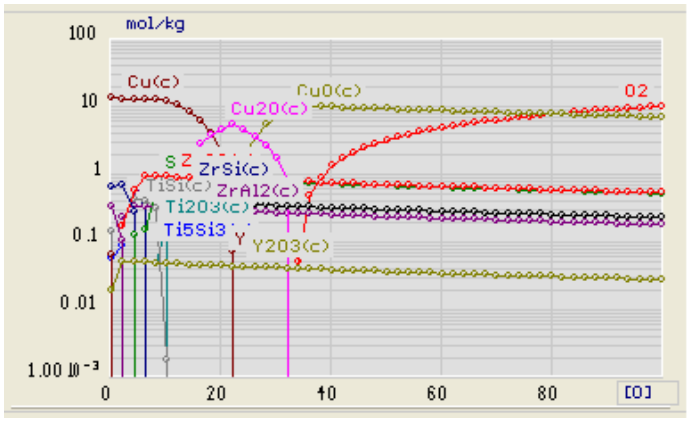

Figure 35 TERRA Analysis for Copper ABA Indicating Alloy Formation

Figure 36 depicts the various titanium oxides that form as a function of oxygen partial pressure. As oxygen partial pressure decreases throughout the internal structure of the braze metal, the titanium oxide could be changing phase. A titanium phase change may be associated with a volumetric change which can cause voids in the internal region of the braze. Titanium exposed to air forms TiO_2. The oxygen concentration decreases from the edge of the braze metal into the interior, which may form the various layers of titanium oxides indicated in the TERRA graph.

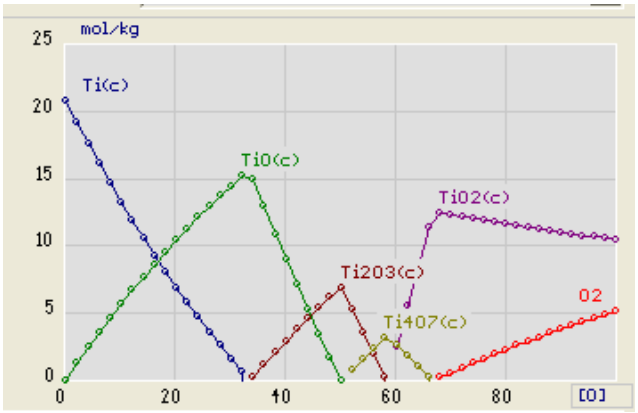

Figure 36 TERRA Analysis Indicating the Formation of Titanium Oxides

MSU Fabricated Braze Compositions

Metallic powders were used to make MSU designed braze compositions which were tailored to the needs of SOFC applications. MSU synthesized brazes were based on modifications of the Copper ABA braze powder due to the success in SOFC brazing tests. Table 10 lists the various MSU synthesized braze compositions including the desired weight percent of each metallic powder used in the composition. Multiple batches of each experimental braze were synthesized and tested, therefore, the chart serves only as an approximation of the actual elemental composition, however, each braze batch was prepared to be as close to the desired composition as possible.

Table 10 Composition of MSU In-house Synthesized Braze Powders

	Element	Weight Percent
Copper ABA (Wesgo Materials) MSU1H	Copper	92.75
	Silicon	3.00
	Titanium Hydride	2.25
	Aluminum	2.00
MSU1	Copper	92.75
	Silicon	3.00
	Titanium	2.25
	Aluminum	2.00

The MSU braze compositions were prepared on the basis to evaluate the effectiveness of brazes prepared with elemental powders and alloyed in-situ (Copper ABA is supplied as a powdered alloy) during the braze process thus allowing a means to optimize braze characteristics.

A braze joint was deemed successful on the basis of two initial criteria: substantial adherence to the YSZ surface and formation of a metallic joint free of large

voids. Braze compositions displaying fracture patterns in which fracture occurred approximately 90% through the YSZ disk and had a cross-section which was mostly free of voids visible to the human eye were regarded as successful and considered for further investigation.

MSU1H

The MSU1H braze composition was designed to be a replica of the Copper ABA commercial braze. According to compositional information of the Copper ABA braze, courtesy of Wesgo Materials, Copper ABA contains 92.75 weight percent copper, 3.00 weight percent silicon, 2.25 weight percent TiH_2 and 2.00 weight percent aluminum.[17] MSU1H was synthesized to compare the performance of an alloyed braze powder (Copper ABA) to that of an in-house synthesized braze powder.

Figure 37 shows a sample brazed using the MSU1H braze paste. While the metallic braze appears to be free of large internal voids, fracture of the sample occurred entirely at the YSZ/Braze interface indicating that a bond was not achieved between the metallic braze and the ceramic. After multiple unsuccessful iterations, this braze composition was determined unsuccessful and discontinued from further study.

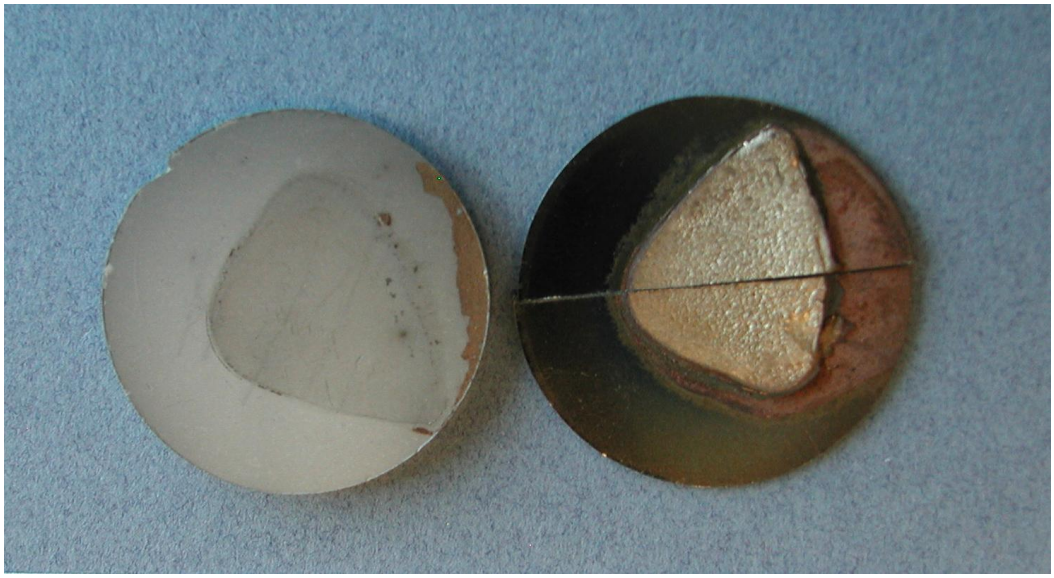

Figure 37 MSU1H Vacuum Braze Joint

MSU1

In the MSU1 braze composition Titanium-hydride was replaced with pure titanium powder. It is uncertain whether the titanium in the commercial braze composition is actually that of titanium-hydride or pure titanium metal, so this braze was also used as a comparison to the commercial braze, Copper ABA.

The MSU1 braze paste was tested in both a vacuum and an argon environment. Figure 38 shows an MSU1 sample brazed in a vacuum environment. The metallic braze appears to be free of large voids, however, fracture has occurred primarily at the YSZ/braze interface, with a small portion occurring through the YSZ disk. This fracture pattern indicates a partial bond between the ceramic and the metallic braze. Partial bonding suggests that this braze composition could be investigated further in the future.

Figure 38 MSU1 Vacuum Braze Joint

Figure 39 shows an MSU1 sample brazed in an argon gas environment. The metallic braze shows large voids throughout and has fractured partially through the YSZ disk and partially at the YSZ/braze interface. The fracture pattern indicates partial bonding. The portion of the braze paste that did not bond could be the result of improper wetting in that region or residual oxygen in the brazing chamber.

Figure 39 MSU1 Argon Braze Joint

The bonded portion of the MSU1 vacuum braze joint was mounted, polished and examined with EDS. Figure 40 shows an EDS line-scan indicating a build-up of titanium and silicon clusters at the stainless steel/braze interface, this pattern was also detected in the EDS line-scans for the Copper ABA braze joint. The partially bonded vacuum braze tests and similar line-scan images obtained with the MSU1 braze paste suggest a possible mimic of the Copper ABA commercial braze.

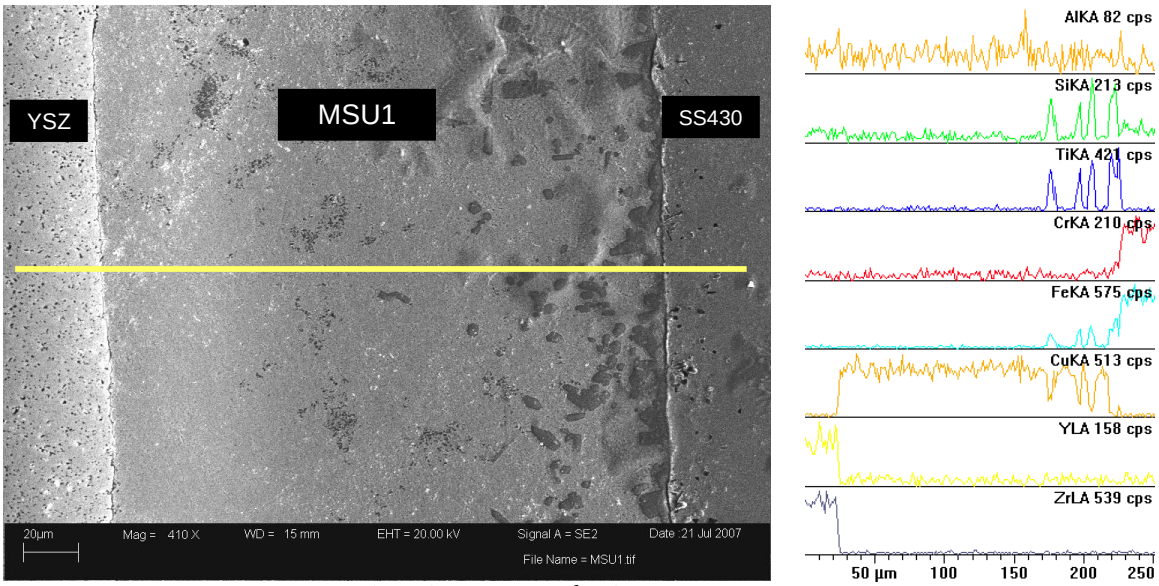

Figure 40 EDS Line-scan of MSU1 Vacuum Braze Joint

Due to the excessive amount of voids in the MSU1 argon brazes and the mediocre bonding characteristics of the MSU1 vacuum brazes, this braze composition was discontinued from additional research tests.

MSU Silicon-Free Fabricated Braze Compositions

In the remaining MSU braze compositions silicon powder was removed and replaced with other base elements from the Copper ABA braze composition. This change

was made after FEM analysis indicated silicon diffusion into the YSZ substrate. As previously stated, the presence of silicon in the electrolyte of the cell is believed to lead to fuel cell degradation, significantly decreasing the operating life of the SOFC. In an effort to avoid the potential problems of silicon diffusion, the MSU silicon-free braze pastes were developed. Compositional information for the silicon-free brazes are shown in Table 11.

Table 11 Composition of MSU Silicon-Free In-house Synthesized Braze Powders

	Element	Weight Percent
MSU2	Copper	95.75
	Titanium	2.25
	Aluminum	2.00
MSU3	Copper	92.75
	Titanium	2.25
	Aluminum	2.00
MSU4	Copper	92.75
	Titanium	5.25
	Aluminum	2.00
MSU5	Copper	92.75
	Titanium	3.75
	Aluminum	3.50
MSU6	Copper	92.75
	Aluminum Titanate	3.00
	Titanium	2.25
	Aluminum	2.00

MSU2

A sample brazed with the MSU2 braze paste is shown in Figure 41. This sample shows a large void throughout the interior of the metallic braze with fracture of the braze sample occurring primarily at the YSZ/braze interface. The sample indicates the best test

results obtained with the MSU2 braze composition and further research was not implemented using this composition.

Figure 41 MSU2 Vacuum Braze Joint

MSU3

The MSU3 braze was designed after experimental tests with the MSU2 braze proved to be unsuccessful. FEM analysis of previous brazes indicate increased regions of aluminum and titanium at the YSZ/braze and braze/stainless steel interfaces. These increased regions of aluminum and titanium are believed to aid in the bonding of the metallic braze to the outlying SOFC components. For the MSU3 braze composition, the silicon was replaced with aluminum to aid in the bonding between the YSZ and the metallic braze.

Figure 42 MSU3 Vacuum Braze Joint

Figure 42 shows a sample brazed in vacuum using the MSU3 braze paste. Fracture of the sample occurred almost entirely through the YSZ disk. There are no regions of outlying braze which did not bond to the ceramic. Most of the MSU3 samples fractured in the same way as the sample shown above. The cross-section of the MSU3 braze was free of voids visible to the human eye. The MSU3 braze is currently the most successful MSU developed braze and will be discussed in more detail later in this paper.

MSU4

In the MSU4 braze silicon was replaced with titanium. While test runs of the MSU3 braze proved the feasibility of a silicon-free braze, the high CTE of the braze compositions was still a primary concern. Since titanium yields the potential to form a graded oxide layer, titanium was used in place of the silicon in the MSU4 braze as the graded oxide layer may help mitigate stresses induced due to the CTE mismatch.

Figure 43 MSU4 Vacuum Braze Joint

The fracture pattern displayed in Figure 43 indicates fair bonding of the MSU4 braze composition with fracture occurring primarily through the YSZ disk and partially at the YSZ/braze interface. While the MSU4 braze composition did bond to most of the ceramic disk, the cross-section showed minor internal voids throughout the joint. The MSU4 braze composition was not subjected to further investigation as it was not bonding quite as well as the MSU3 braze, but would be a strong candidate for additional testing in the future.

MSU5

In the MSU5 braze paste the silicon was replaced with equal amounts of aluminum and titanium (1.5 weight percent of each). The aluminum was used to help aid in the bonding of the metallic braze to the YSZ and the titanium was used to possibly help mitigate the CTE mismatch between the braze and the SOFC components.

Figure 44 MSU5 Vacuum Braze Joint

Figure 44 shows the fracture pattern for the MSU5 vacuum braze joint. The braze joint appears to be free of large internal voids, with fracture of the sample occurring partially through the YSZ disk and partially at the YSZ/braze interface. Since the sample only exhibited partial bonding, further testing was not conducted; however, this composition may be investigated further in the future.

MSU6

In the MSU6 braze composition silicon was replaced with aluminum titanate (ALT). ALT was a desired braze additive due to its extremely low CTE, which may aid in the reduction of residual stresses that could be seen in an operating SOFC. ALT was also desirable as it contains both aluminum and titanium which appear to aid in the bonding process, however, as the two elements are alloyed into ALT, they may react differently during the brazing process, making MSU6 a worthwhile braze composition for experimental studies.

Figure 45 MSU6 Vacuum Braze Joint

Figure 45 shows the fracture pattern for the MSU6 vacuum braze joint. The metallic braze has large regions of internal voids throughout the joint with fracture of the sample has occurring entirely at the YSZ/braze interface. This composition was deemed unsuccessful and further testing was not conducted.

MSU3 In-House Synthesized Alloy

The in-house synthesized braze composition that gave the best overall results was the MSU3 in-house braze which consists of 92.75 weight percent copper, 2.25 weight percent titanium and 5.00 weight percent aluminum. Due to the good performance of this braze composition, additional investigation was given to this braze over the other MSU in-house synthesized compositions.

FEM and EDS Data

FEM was used to examine the micro-structural and compositional behavior at the interface between the metallic braze and the ceramic as well as between the metallic braze and the stainless steel. EDS line scans were performed to obtained qualitative information regarding the distribution of each individual element within the metallic brazes to better understand the bonding mechanisms of the brazing material.

Vacuum Tests: Figure 46 shows an EDS line scan of a cross-sectioned YSZ disk joined to a 440 stainless steel disk using an in-house synthesized, silicon-free braze paste identified as MSU 3. The MSU3 braze does not appear as homogenous as the Copper ABA braze. This could be the result of inadequate mixing of the braze with the ultra-sonic mixer. A more robust mixing procedure may help improve the braze homogeneity.

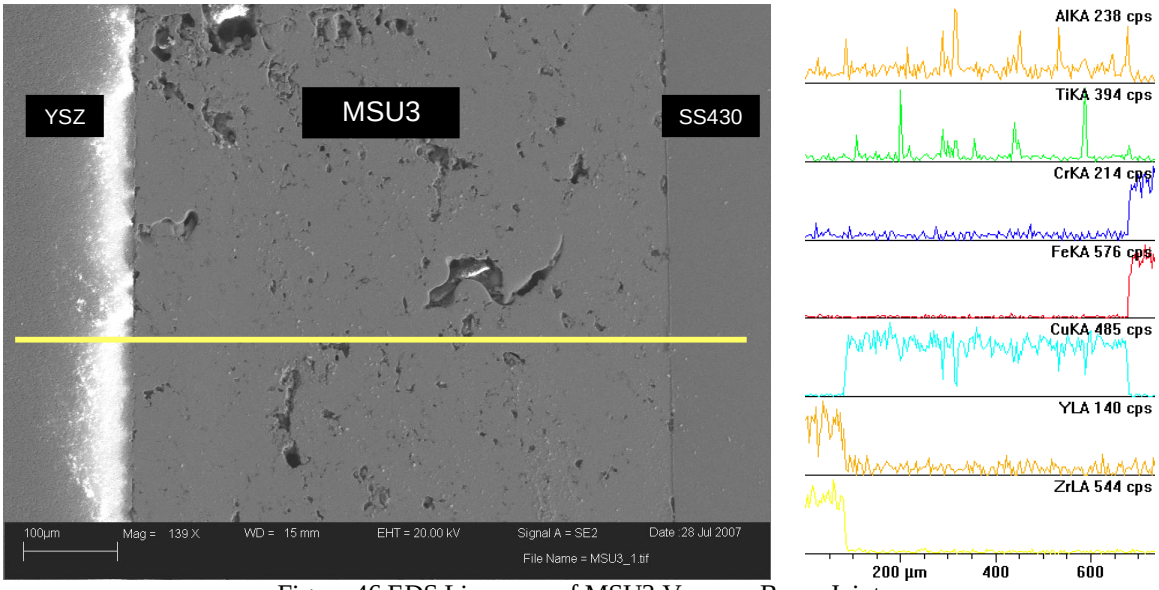

Figure 46 EDS Line-scan of MSU3 Vacuum Braze Joint

FEM microscopy shows small voids in the bulk of the braze material which could potentially affect the hermetic nature of the braze seal. The small voids which appear in the braze metal could be from trapped air in the braze which was not completely removed during the vacuuming of the braze chamber.

EDS detected small titanium, and aluminum peaks at both braze interfaces, which can be seen in Figure 47 and Figure 48, indicating a chemical bond.

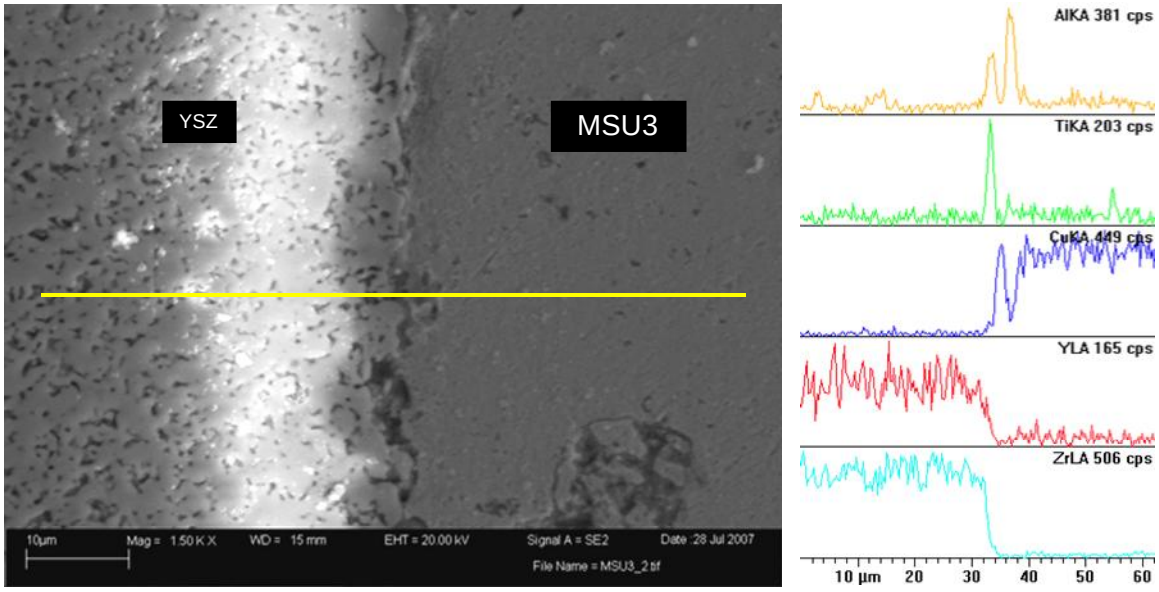

Figure 47 EDS Line-Scan for YSZ/Braze Joint Interface for MSU3

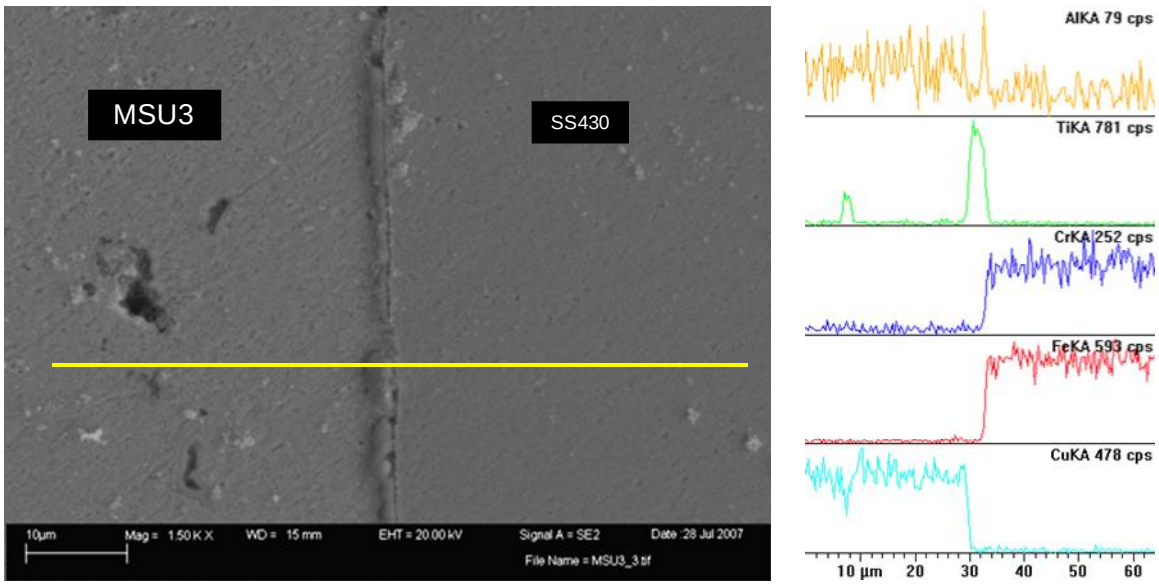

Figure 48 EDS Line-scan for Braze/SS Joint Interface for MSU3

Argon Tests: Brazing tests conducted in an Argon gas environment did not perform as well as those conducted in a vacuum environment. Figure 49 shows a braze joint that has been pried apart between the ceramic and steel disks. Fracture of the joint has occurred primarily between the YSZ/braze interface. Most of the ceramic has remained bonded to the braze interface, however, not the complete bonding as shown with the vacuum braze pieces.

Figure 49 Fracture Pattern of MSU3 Argon Braze Joint

Pop-Gun Tests

Figure 50 depicts a rupture test cup after a completed test with the MSU3 in-house metallic vacuum braze. As can be seen, fracture of the sample occurred primarily through the YSZ disk, indicating a good bond between the ceramic and the metallic braze.

Figure 50 Pressurized Rupture Test Cup for MSU3 Alloy Brazed in Vacuum

A successful braze is proven by the results of the rupture test conducted at room temperature which is shown in Figure 51. The MSU3 in-house braze was able to withstand pressures of up to 150 psi before fracture, well above the strength needed to SOFC applications. The formation of a hermetic seal has yet to be obtained with the MSU3 in-house synthesized braze.

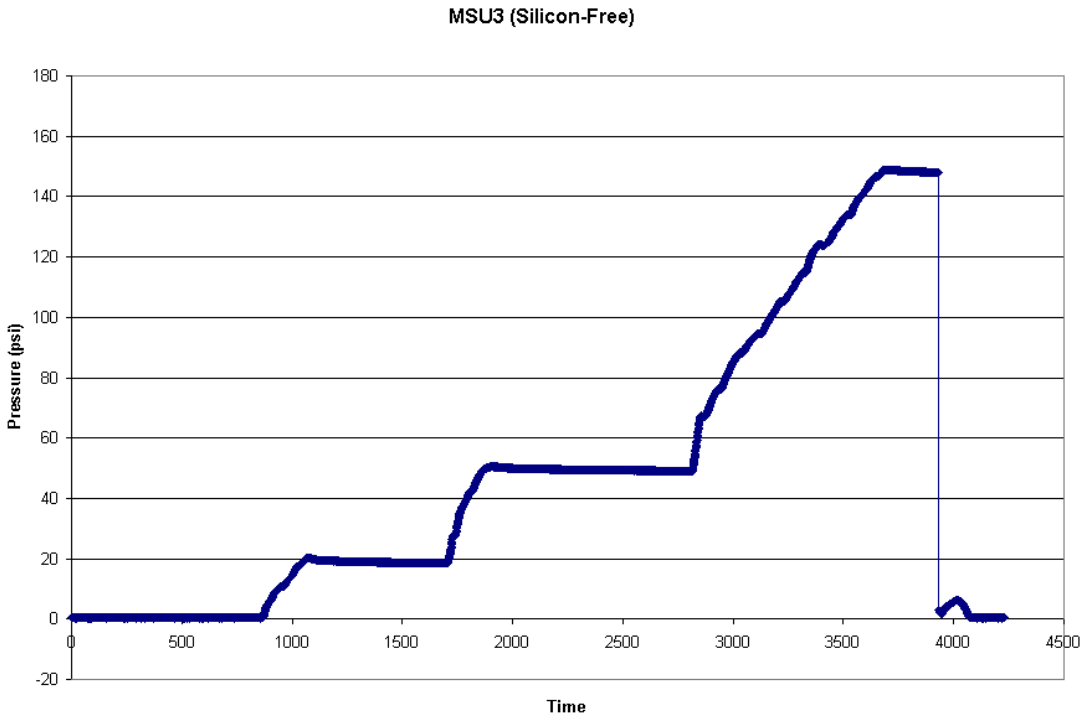

Figure 51 Pressurized Rupture Test Results for MSU3

DTA Analysis

A DTA study was conducted in forming gas (5% hydrogen, balance nitrogen) to a temperature of 1200 °C for the MSU3 in-house braze powder. The braze powder was subject to an increase in temperature at 10°C per minute up to 1200°C, the temperature was then held at 1200°C for 15 minutes. Finally, the chamber was cooled at 20°C per min down to room temperature.

The DTA results, shown in Figure 52, indicate two exothermic peaks occurring at 337.3°C and 582.8°C. These peaks are unidentified at this time, but are hypothesized to be points at which alloys are forming between the elements in the braze powder. Since the MSU3 powder is synthesized at MSU, the powder is in the form of individual

elements and it is possible that these elements may be forming inter-metallic alloys at the elevated temperatures.

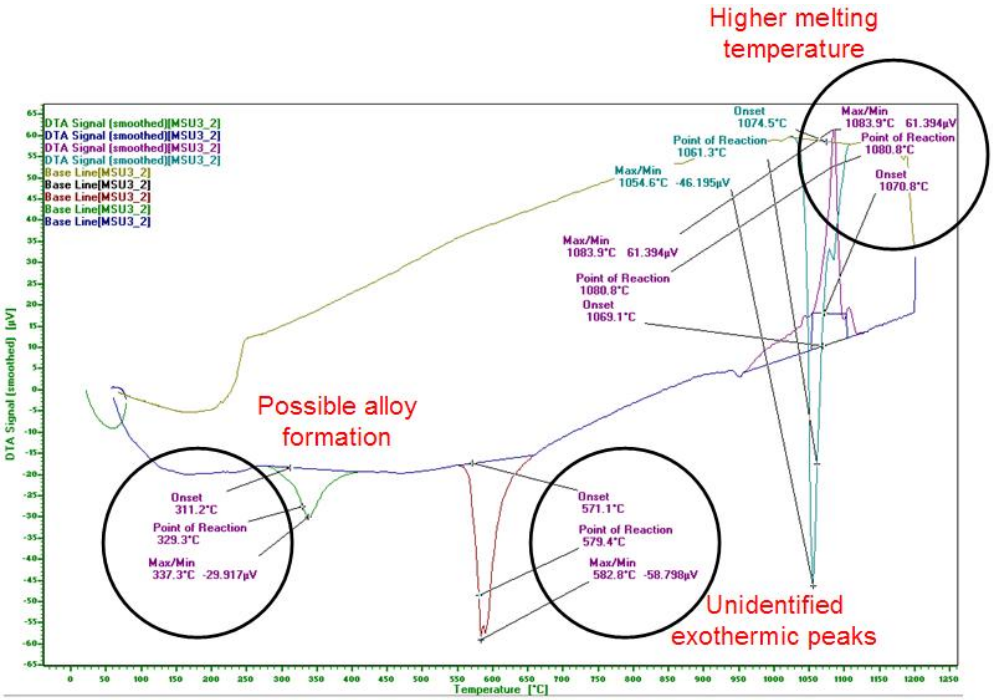

Figure 52 DTA Results of MSU3 Braze in Forming Gas

DTA shows an endothermic peak occurring at 1083.9 °C, indicating the liquidus melting temperature for the MSU3 in-house braze powder. This melting temperature is much higher than the melting temperature for the Copper ABA brazing powder, which is 1024°C. The increase in melting temperature is most likely the result of removing the silicon from the braze powder composition. According to the Copper-silicon phase diagram, shown in Figure 8, it looks as though small additions of silicon will have a significant effect on the melting temperature of the brazing powder.

The final exothermic peak, occurring at 1054.6°C, indicates the re-solidification of the brazing powder from liquid to solid phase. As previously stated, the melting and solidification points of the peaks do not typically correspond due to the fact that melting

can occur homogeneously, however, crystallization can be suppressed by rapid cooling and lack of good heterogeneous nucleation sites.

TGA Analysis

TGA of the MSU3 in-house braze alloy has not been conducted at this time.

TERRA

Figure 53 is a plot depicting the possible reactions occurring between the YSZ and the braze metal as a function of oxygen partial pressure. The results indicated in this TERRA plot are very similar to those presented in the TERRA plot of the Copper ABA braze only silicon has been removed. This figure again indicates the formation of an aluminum oxide followed by the formation of a titanium oxide; however, the silicon oxide is no longer indicated.

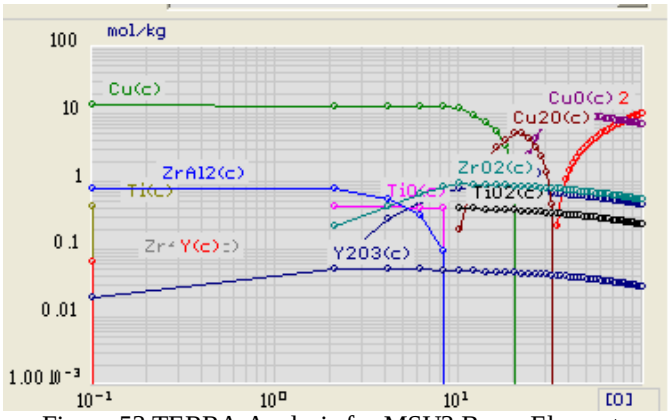

Figure 53 TERRA Analysis for MSU3 Braze Elements

The formation of various inter-metallic alloys is again indicated by the TERRA program. In the case of the MSU3 braze, the TiSi inter-metallic alloy is no longer present and this can be confirmed by the lack of TiSi clusters in the FEM images of the interior of the braze metal.

MSU3 Atomized Alloy

The MSU3 atomized alloy was atomized by HJE Company Inc [27]. The atomized alloy follows the recipe of the designed MSU3 in-house braze powder and consists of 92.75 weight percent copper, 5.0 weight percent aluminum and 2.25 weight percent titanium. The powder is -325 mesh with a mean particle size of 21.7 micron and a standard deviation of 11.8 micron.

Figure 54 shows the fracture pattern for the MSU3 atomized brazing alloy brazed at 1100 °C. Fracture of the sample occurred primarily at the YSZ/braze interface, indicating a poor bond. Despite the poor performance of the MSU3 atomized alloy, additional sample characterization was done to understand the elemental distribution throughout the alloy in an effort to obtain better performance.

Figure 54 Fracture Pattern for MSU3 Atomized Alloy

FEM and EDS Data

FEM was used to examine the micro-structural and compositional behavior at the interface between the metallic braze and the ceramic as well as between the metallic braze and the stainless steel. EDS line scans were performed to obtained qualitative information regarding the distribution of each individual element within the metallic brazes to better understand the bonding mechanisms of the brazing material.

Vacuum Tests: Figure 55 shows an EDS line scan of a cross-sectioned sample of a YSZ disk joined to a 430 stainless steel disk using the MSU3 atomized alloy, silicon-free braze. While the YSZ disk is present in the image, a majority of the ceramic did not bond with the metallic braze. The ceramic portion indicated in the FEM image represents only a small portion of the sample.

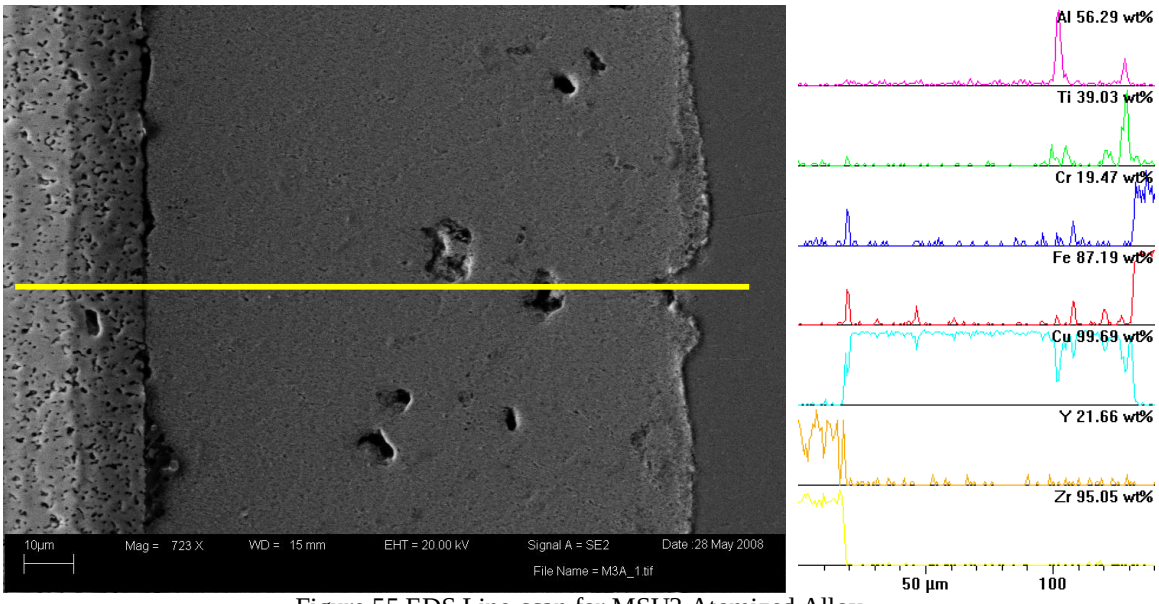

Figure 55 EDS Line-scan for MSU3 Atomized Alloy

FEM analysis shows that the atomized brazing alloy is much more homogenous than the in-house synthesized version, indicating a better mixing process. There appears

to be evidence of an iron and chromium peak at the YSZ/braze interface and a small peak located within the interior of the braze. It is possible that these peak corresponds to a small sample of stainless steel that was pulled to the braze side during polishing of the mounted sample.

EDS detected small titanium and aluminum peaks at the YSZ/braze interface as well as the stainless steel/braze interface, which are shown in Figure 56 and Figure 57, respectively.

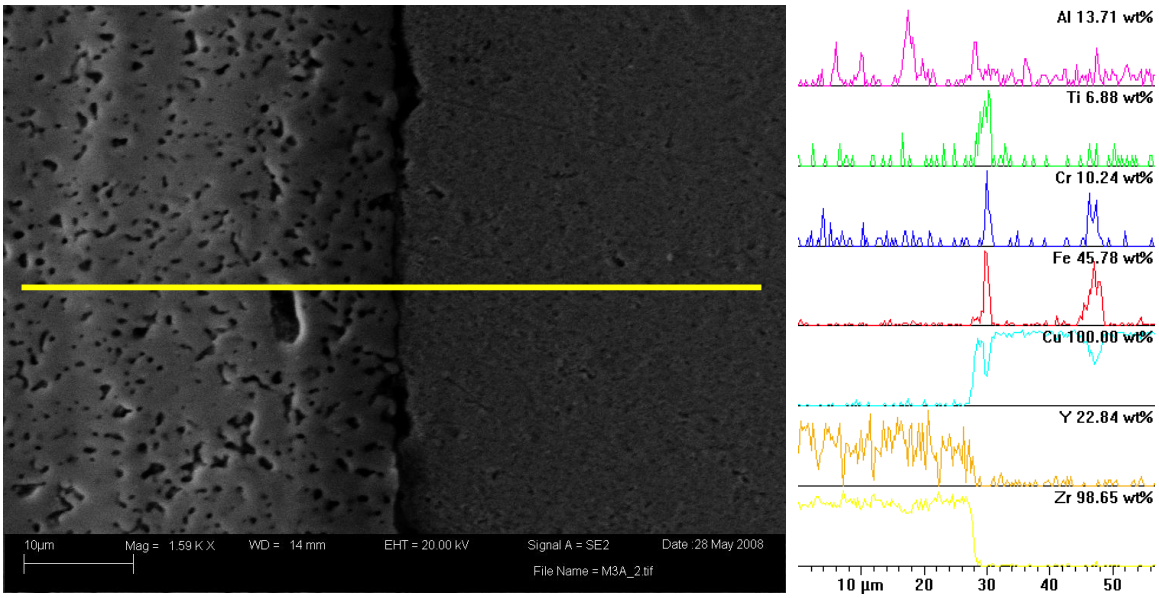

Figure 56 EDS Line-scan for YSZ/Braze Interface of MSU3 Atomized Alloy

EDS detects only minor peaks of titanium and aluminum at the YSZ/braze interface which may be the reason for the poor bonding between the YSZ/braze interface. It is believed that the atomization process has “locked-up” the titanium with the other braze elements. This prevents the titanium from migrating to the braze interface, thus prohibiting the titanium from reacting with the YSZ. This may suggest that the titanium hydride in the Copper ABA braze is added after the alloying process, leaving the titanium free to migrate during the brazing process.

The indication of iron and chromium at the YSZ/braze interface is not a typical result and is under further investigation. EDS of the stainless steel/braze interface yield results similar to previously successful braze alloys. A small cluster appears to the left of the interface indicated as primarily titanium and a small amount of aluminum. Clusters of this nature also appear in the MSU3 in-house alloy, but in greater number.

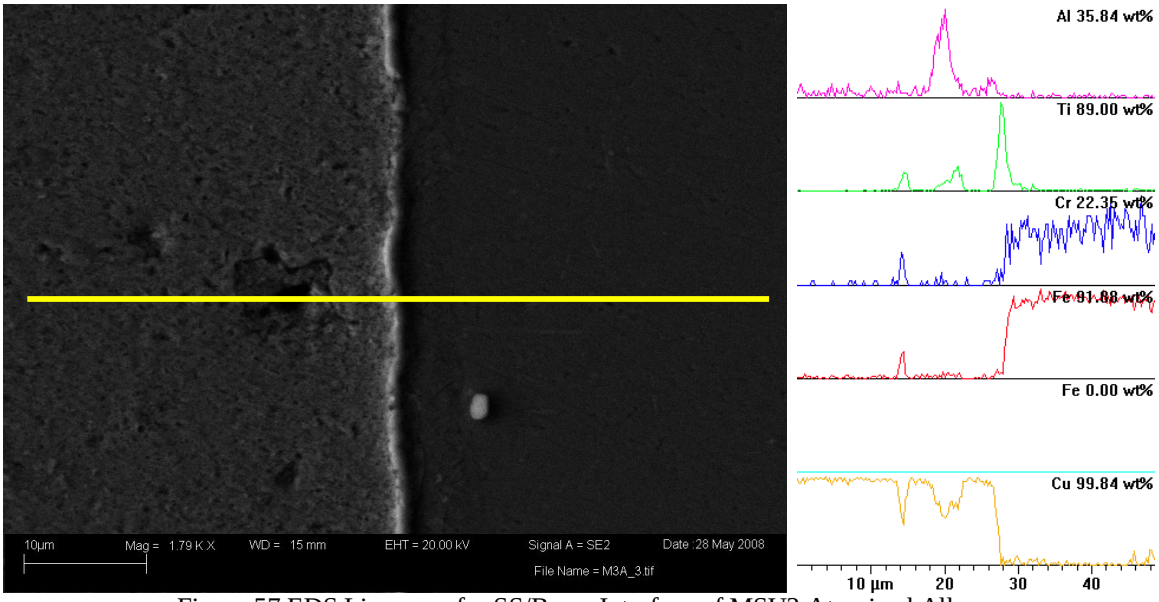

Figure 57 EDS Line-scan for SS/Braze Interface of MSU3 Atomized Alloy

Argon Tests: Due to the fact that the MSU3 atomized alloy is not performing well in the vacuum brazing tests, Argon braze tests have yet to be conducted.

Pop-Gun Tests

Figure 58 shows the results of a pressurized rupture test conducted at room temperature for the MSU3 atomized braze alloy. It can be seen that the MSU3 atomized braze is not able to withstand pressures equal to those achieved with the Copper ABA and MSU3 in-house brazes. The maximum pressure reached with the MSU3 atomized alloy is approximately 32 psi, at present time. Again, the poor bonding and strength

characteristics may be the result of the titanium being “locked-up” in the atomized brazing alloy.

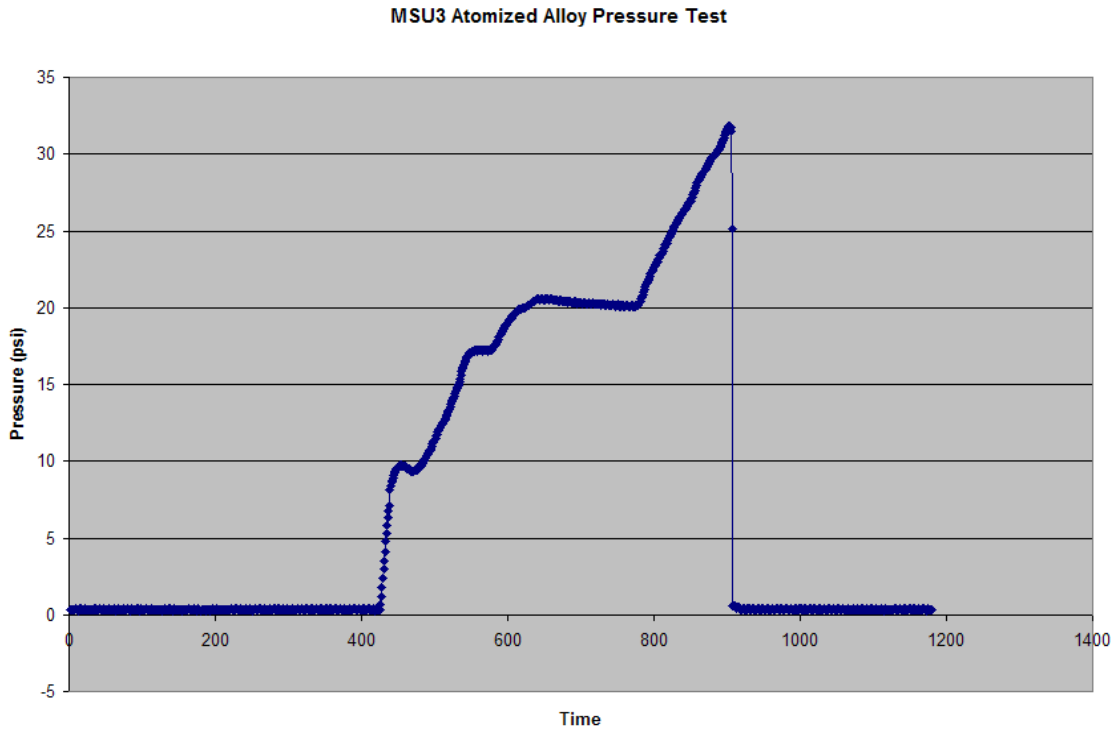

Figure 58 Pressurized Rupture Test Results for MSU3 Atomized Alloy

DTA Analysis

A DTA study was conducted in forming gas (5% hydrogen, balance nitrogen) to a temperature of 1200 °C for the MSU3 atomized alloy braze powder. The braze powder was subjected to an increase in temperature at 10°C per minute up to 1200°C, the temperature was then held at 1200°C for 15 minutes. Finally, the chamber was cooled at 20 °C per min down to room temperature.

The DTA results, shown in Figure 59, indicate an endothermic peak occurring at 548.0°C. The cause of this peak is unknown at this time; however, a similar peak was noticed in the DTA results for the Copper ABA brazing powder, occurring at a slightly

higher temperature of 672.1 °C. In the case of the Copper ABA braze powder, this peak was believed to correspond with hydrogen desorption due to the titanium hydride. The MSU3 atomized alloy does not contain titanium hydride, thus, further research will need to be conducted in order to determine the endothermic peak for the MSU3 atomized alloy as well as to confirm or reject the theory for the endothermic peak corresponding to the Copper ABA brazing powder. However, the endothermic peak could be due to the burnout of residual moisture in the TGA chamber.

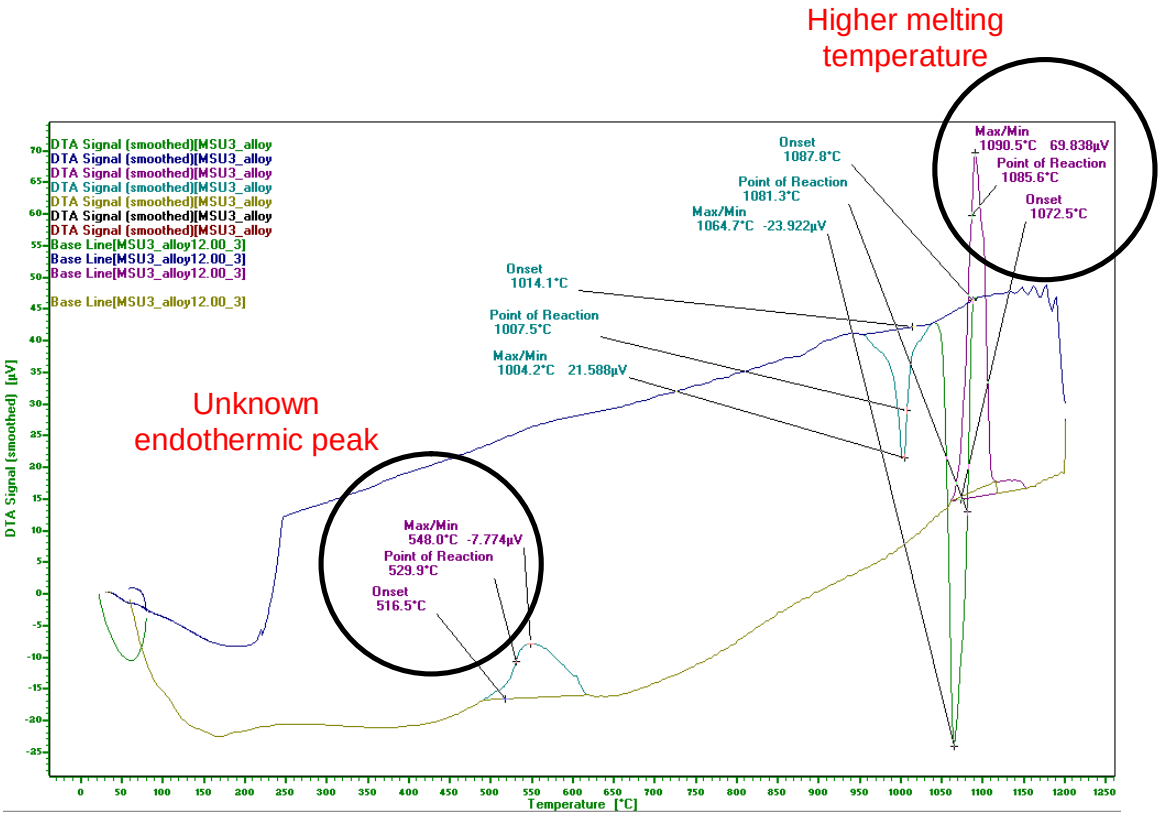

Figure 59 DTA Results of MSU3 Atomized Alloy in Forming Gas

DTA indicates a second endothermic peak occurring at 1090.5°C, specifying the liquidus melting temperature for the MSU3 atomized braze powder. As was the case with the MSU3 in-house synthesized brazing powder, the melting temperature for the

MSU3 atomized alloy is much higher than the melting temperature for the Copper ABA brazing powder, which is 1024°C. The melting temperature for the MSU3 atomized alloy is comparable to the melting temperature for the MSU3 in-house braze powder. Due to the fact the both the in-house MSU3 braze powder and the atomized MSU3 braze powder are comprised of the same ratio of elements, the similar braze melting temperatures are expected. Additionally, the higher melting temperature for the MSU3 atomized alloy is believed to be the result of the silicon removal as was case for the MSU3 in-house braze powder.

DTA indicates two exothermic peaks occurring during the cool down for the MSU3 atomized alloy. The first endothermic peak, occurring at 1064.7°C, is believed to indicate the re-solidification of the brazing powder from liquid to solid phase. However, the cause of the second endothermic peak, occurring at 1004.2°C, is unidentified at this time.

TGA Analysis

A TGA test has yet to be conducted for the MSU3 atomized braze alloy.

TERRA

The TERRA results for the MSU3 atomized braze alloy are identical to the results for the MSU3 in-house synthesized braze as they are composed of the same amount of the same elements.

Coefficient of Thermal Expansion Matching

As previously stated, the CTE mismatch between the braze metal and the SOFC components is a key challenge in the successful development of SOFC stacks. The CTE of the Copper ABA braze powder is 19.5×10^{-6}/°C, which is significantly higher than the CTE for the YSZ and the stainless steel which are 9.5×10^{-6}/°C and 12.7×10^{-6}/°C, respectively. In an effort to address the CTE mismatch between the metallic braze and the adjoining SOFC materials, small amounts of Aluminum Titanium Oxide (Al_2TiO_5, ALT), with a CTE of 0.67×10^{-6} /°C, was added to the braze powders.

An approximation of the new CTE for the braze powder with the ALT addition can be calculated using the rule of mixtures (ROM).

$$\alpha_c = \alpha_r \times V_r + \alpha_m \times V_m$$

Equation 10 Calculation for CTE [26]

where α_c is the CTE of the composite, V_m is the volume percent of the matrix phase, α_r is the CTE of the reinforcement and V_r is the volume percent of the reinforcement phase.

FEM and EDS Data

FEM was used to examine the micro-structural and compositional behavior at the interface between the metallic braze and the ceramic as well as between the metallic braze and the stainless steel. EDS line scans were performed to obtained qualitative information regarding the distribution of each individual element within the metallic brazes to better understand the bonding mechanisms of the brazing material.

Vacuum Tests: Vacuum brazing tests conducted with the MSU3 in-house braze alloy including the addition of ALT proved to be successful. Figure 60 shows a braze sample which was pried apart between the YSZ and stainless steel disks. The fracture appears to have occurred primarily throughout the YSZ disk, indicating a strong bond between the metallic braze and the ceramic.

Figure 60 Fracture Pattern for MSU3 In-House with the Addition of ALT

Figure 61 shows an EDS line scan for an MSU3 in-house synthesized braze joint in which approximately one weight percent of ALT has been added to the original MSU3 in-house synthesized brazing powder. Large clusters of ALT appear throughout the interior of the braze indicating that a more robust mixing procedure may be necessary to obtain a homogeneous braze paste, especially when introducing the ALT additive.

The MSU3 braze powder bonds well with the addition of the ALT. Aluminum and titanium peaks are present at both braze interfaces as was shown with EDS analysis

of the original MSU3 in-house braze. This yields a well-bonding braze, with the possibility of CTE manipulation through the addition of ALT.

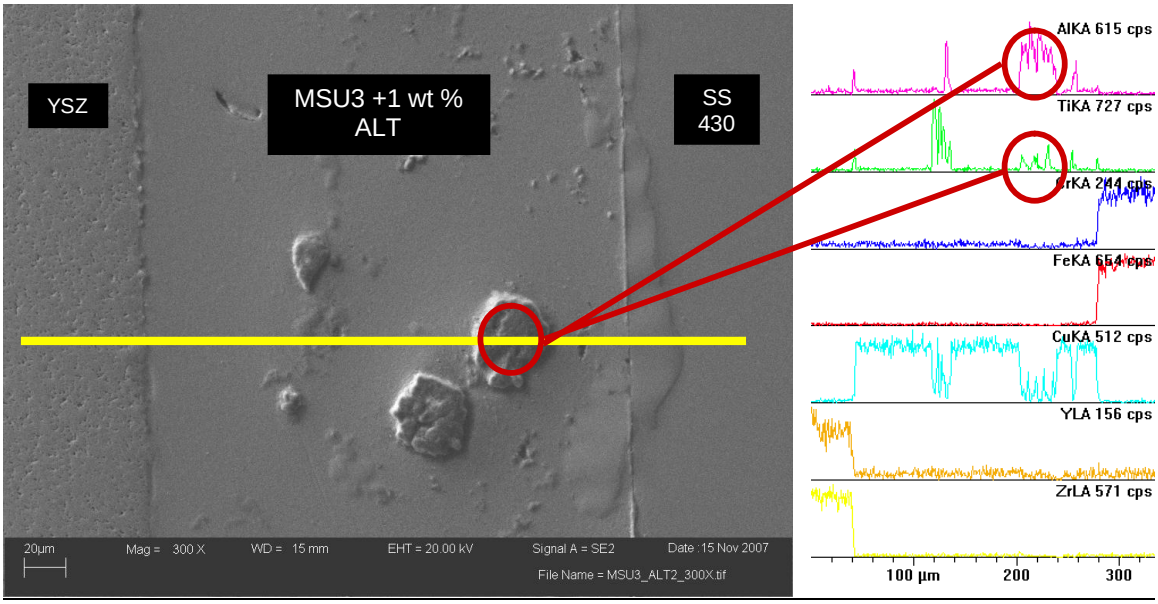

Figure 61 EDS Line-scan of Vacuum MSU3 Braze Joint with ALT Addition

Argon Tests: Braze test of the MSU3 in-house alloy with the addition of ALT have yet to be conducted.

Pop-Gun Tests

Figure 62 shows the results of a pressurized rupture test conducted at room temperature for the MSU3 in-house synthesized braze alloy with the addition of approximately one weight percent ALT. The maximum pressure reached with this new braze alloy was approximately 150 psi, indicating that the integrity of the braze seal was maintained despite the addition of the ALT. This means that ALT could be an effective additive for reducing the overall CTE of the brazing alloy while maintaining the desired bonding and strength properties of the original braze.

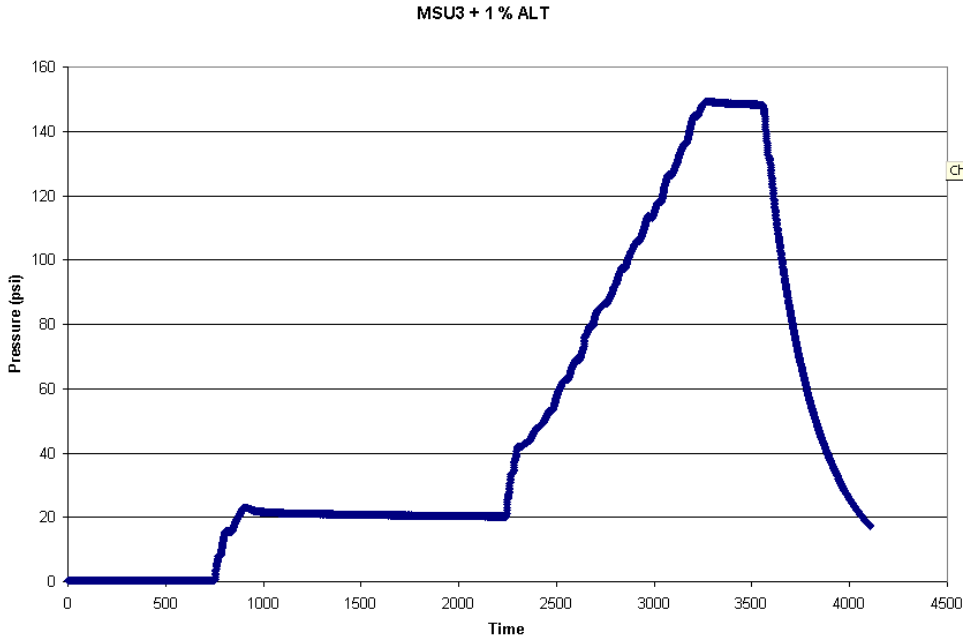

Figure 62 Pressurized Rupture Test Results for MSU3+ALT

CONCLUSIONS

Summary of Results

Robust copper-based brazes show potential for the use of hermetic sealing in SOFC applications. The metallic brazes were characterized by differential thermal analysis, oxidation characteristics, FEM/EDS analysis, thermodynamic simulations, pressurized strength tests and hermeticity. While evidence of silicon diffusion into the YSZ may be problematic for long-term SOFC operations, the brazes display desirable characteristics for brazing applications including the formation of chemically bonded braze joints, formation of a protective aluminum oxide barrier and hermetic, high strength properties that indicate potential for use in SOFC applications.

The deleterious effects of silicon in SOFCs in addition to the results that suggest silicon does not facilitate bonding, oxidation resistance, or improved mechanical properties led to the development of a silicon-free braze. The silicon-free braze has yielded excellent performance near that of the commercially available Copper ABA, proving to form robust joints with stainless steel and YSZ.

It is apparent that the active element, titanium, plays a very important role in the bonding of the ceramic to the braze. The braze does not bond well if the titanium is "locked-up" as is the case for the MSU3 atomized alloy. The MSU3 in-house synthesized braze powder utilizes free titanium allowing for titanium migration to the braze/YSZ interface, thus providing the active element needed to form a chemical bond. The "locked-up" titanium in the MSU3 atomized braze is not free to migrate the braze/YSZ interface, giving poor performance. While high braze melting temperature is

a concern, possible metal additives in the form of Mg or ALT give way to potential lower temperature, silicon-free brazing alloys.

Future Work

Due to the success shown for active metal copper-based brazing, the development of a copper-based braze specifically tailored for SOFC applications is a desired future goal. While MSU tailored metallic brazes are showing promise as robust seals for SOFC stacks, many parameters still need to be optimized. Braze characteristics which should remain under investigation include: lowering the CTE of the metallic braze composition, lowering the brazing temperature of the metallic alloy, producing an alloy which brazes well in both a mid-level vacuum and inert argon-gas environment, shows high strength characteristics at elevated temperature, and has no poisonous, or degrading effects on other cell components.

As a result of the successful performance of the MSU3 in-house synthesized braze alloy, development of additional silicon-free brazes which meet other needs of the braze seal requirements including CTE matching and brazing temperature reduction are recommended. Such compositions should utilizes alternative metals which would yield lower braze melting temperature. Additionally, previously studied silicon-free braze compositions should be further investigated.

Due to the poor performance of the MSU3 atomized brazing alloy, additional studies are encouraged utilizing the brazing powder. Current investigations utilizing additions of titanium-hydride have shown initial success. Studies should focus on

determining the optimal amount of Titanium-hydride necessary for robust braze seals in addition to working with CTE reduction and braze temperature reduction. This study could also incorporate the investigation of ALT additions which have shown promising results in reducing the overall CTE of the brazing alloy.

High temperature rupture tests need be conducted to analyze the robustness of the brazing seals in the range of temperature for typical SOFC operation, primarily 700-900°C. Additionally, it is suggested that a new geometrical configuration for the pop-test be designed to test for a shear-type failure as opposed to the tensile failure which is currently being tested. Finally, performing seal tests on operating SOFC stacks is recommended once an optimized brazing alloy has been synthesized.

REFERENCES

1. Koch, A., H.P. Buchkremer, D. Stoever, D. Stolten, & R. Wilkenhoener. (2001) Brazing of Metallic Conductors onto Ceramic Plates in Solid Oxide Fuel Cells. [Electronic Version]. *Journal of Materials Science*, 36, 1775-1782.

2. Kim, Jin Yong, John S. Hardy, & K. Scott Weil. (2005). Novel Metal-Ceramic Joining for Planar SOFCs. [Electronic Version]. *Journal of the Electrochemical Society*, 152 (6) J52-J58.

3. Buscher, Johannes-Moritz. (2006) Active Brazing Technologies for Planar Solid Oxide Fuel Cell Seals. Technical University of Berlin.

4. F. Furthner. (2006) Optimization of a Micromachined SOFC's Design. [Electronic Version] Cranfield University.

5. Lessing, Paul A. (2007) A Review of Sealing Technologies Applicable to Solid Oxide electrolysis cells, [Electronic Version]. *Journal of Material Science*, 42: 3465-3476.

6. Singh, Raj N. (2007). Sealing Technology for Solid Oxide Fuel Cells (SOFC). [Electronic Version]. *International Journal of Applied Ceramic Technology*, 4 [2] 134-144.

7. Barry, Patrick L. (2007) Upcoming Experiments Planned for the International Space Station will help Engineers on Earth Learn to Handle Commercially-useful Undercooled Fluids. [Online] *National Aeronautics and Space Administration NASA*, 11 June 2008, http://www.nasa.gov/vision/earth/technologies/16oct_viscosity.html.

8. Malzbender, Jurgen, Joseph Monch, Rolf W. Steinbrech, Thomas Koppitz, Sonja M. Gross, & Josef Remmel. (2007) Symmetric Shear Test of Glass-ceramic Sealants at SOFC Operation Temperature. [Electronic Version]. *Journal of Material Science*. 42:6297-6301.

9. Weil, Scott K., Jin Yong Kim, John S. Hardy, & Jens T. Darsell. (2006) The effect of TiO2 on the Wetting Behavior of Silver-Copper Oxide Braze Filler Metals. [Electronic Version] *I Scripta Materials*, 54, 1071-1075.

10. Weil, Scott K., Jin Yong Kim, & John S. Hardy. (2005) Reactive Air Brazing: A Novel Method of Sealing SOFCs and Other Solid-State Electrochemical Devices. [Electronic Version]. *Electrochemical and Solid-State Letters*, 8 (2) A133-A136.

11. Singh, Mrityunjay, Tarah P. Shpargel, & Rajiv Asthana. (2008) Brazing of Yttria-stabilized Zirconia (YSZ) to Stainless Steel using Cu, Ag, and Ti-based Brazes. [Electronic Version]. *Journal of Material Science*, 43:23-32.

12. Singh, M., T.P. Shpargel, & R. Asthana. (2007). Brazing of Stainless Steel to Yttria-Stabilized Zirconia Using Gold-Based Brazes for Solid Oxide Fuel Cell Applications. [Electronic Version]. *International. Journal of Applied Ceramic Technology,* 4 [2] 119-133.

13. Tucker, Michael C., Craig P. Jacobson, Lutgard C. De Jonghe, & Steven J. Visco. (2006). A Braze System for Sealing Metal-supported Solid Oxide Fuel Cells. [Electronic Version]. *Journal of Power Sources,* 160, 1049-1057.

14. Gere, James M. (2004) *Mechanics of Materials Sixth Edition.* Belmont, CA: Brooks/Cole-Thomas Learning.

15. Wikipedia. Wetting. [Online] *Wikimedia Foundation, Inc.*, 11 June 2008. http://en.wikipedia.org/wiki/Wetting

16. de Gennes, P.G. *Wetting: Statics and Dynamics.* College de France, Physique de la Matiere Condensee, 11 Place Marcelin-Berthelot, 75231 Paris Cedex 05, France

17. Morgan Advanced Ceramics, Wesgo Metals. *Wesgo Metals*. [Online] 15 May 2008. http://www.wesgometals.com/

18. Inframat Advanced Materials LLC. 8 mol% Yttria Stabilized Zirconia (YSZ) Powder Superfine Grade. *Inframat Advanced Materials*. [Online] 21 Mar. 2008. http://www.advancedmaterials.us/4039OR-8601.htm.

19. Empower Materials Inc. *Empower Materials Inc*. [Online] 23 Apr. 2007. http://www.empowermaterials.com/

20. Bhadeshia, H. K. D. H. (2002) Thermal Analysis Techniques. University of Cambridge, Materials Science and Metallurgy. [Online] 28 Mar. 2008 http://www.msm.cam.ac.uk/phase-trans/2002/Thermal1.pdf

21. Jacobson, David M., & Giles Humpston. (2005) Principles of Brazing. *ASM International*.

22. Hertz, J. L. (2007). Highly enhanced electrochemical performance of silicon-free platinum–yttria stabilized zirconia interfaces. [Electronic Version] *Journal of Electroceramics.*

23. Brochu, M., B.D. Gauntt, R. Shah, & R.E. Loehman. (2006) Comparison Between Micrometer- and Nano-Scale Glass Composites for Sealing Solid Oxide Fuel Cells. [Electronic Version] *Journal of American Ceramic Society,* 89 [3] 810-816.

24. Mid-Atlantic Casting Services. Understanding Copper-Base Alloys. *Mid-Atlantic Casting* [Online] 15 Apr. 2007. http://www.mid-atlanticcasting.com/copper-base-alloys_FEB05.pdf

25. Sandim, Hugo Ricardo Zschommler, Bruno Viera Morante, & Paulo Atsushi Suzuki, (2005) Kinetics of Thermal Decomposition of Titanium Hydride Powder Using in situ High-temperature X-ray Diffraction (HTXRD), [Electronic Version] *Materials Research*, Vol. 8, No. 3, 293-297.

26. Ashby, Michael, Hugh Shercliff & David Cebon. (2007) *Materials: Engineering, Science, Processing and Design.* Burlington, MA: Elsevier Ltd.

27. HJE Company Inc. *HJE Company Inc.* Montana State University Custom Alloy. 2008